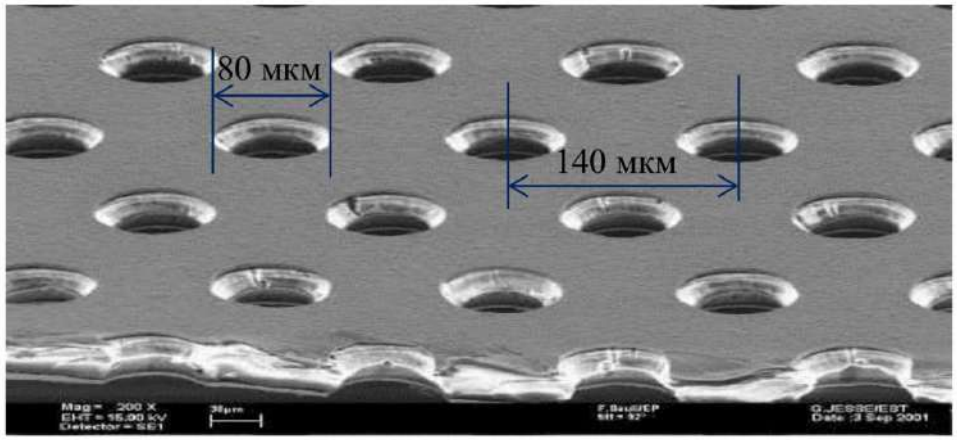

Gas Electron Multiplier detectors for the LHCb experiment

T. Maltsev

24 July 2025

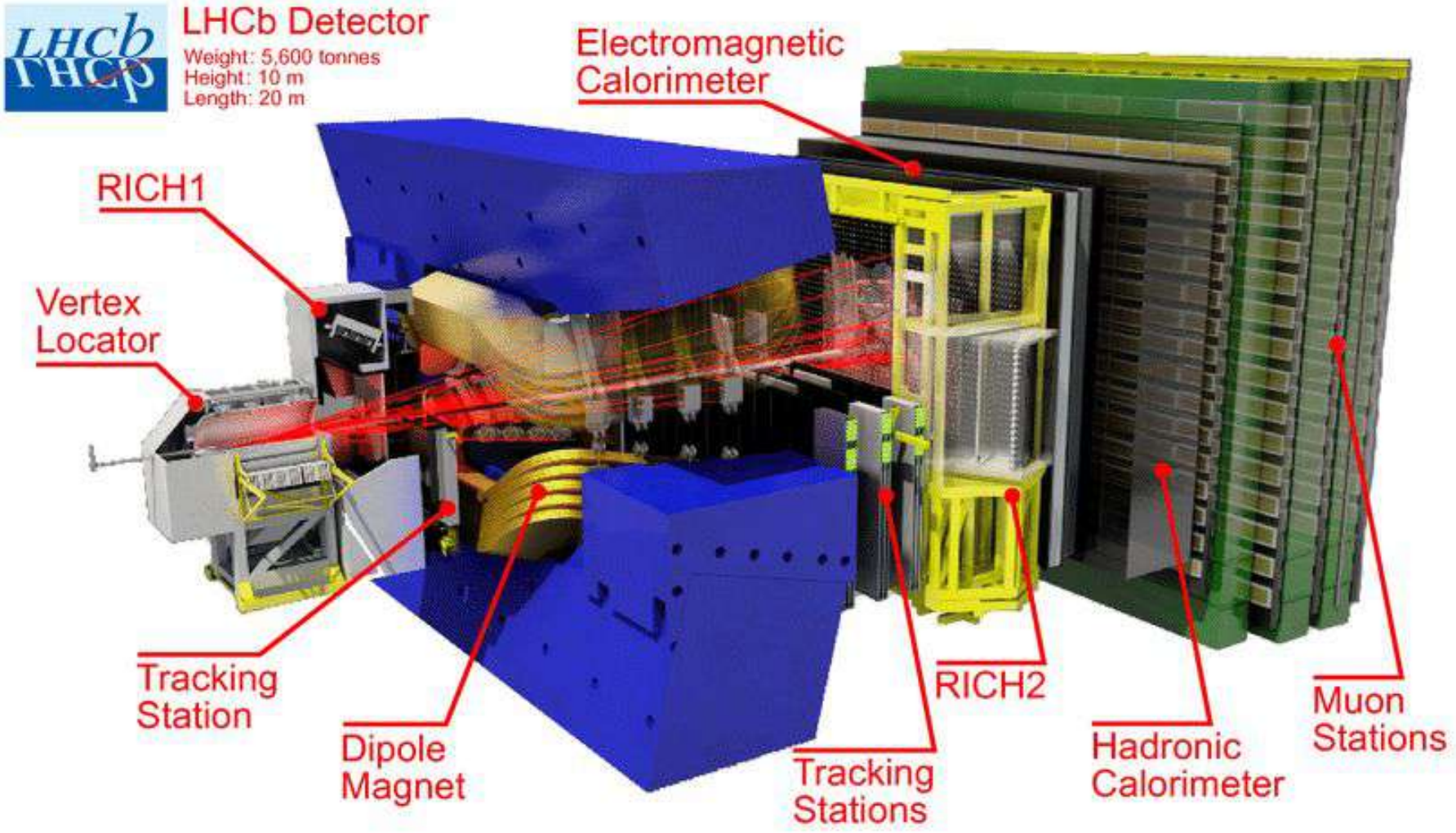

Задача эксперимента LHCb:
исследование эффектов
CP-нарушения
в распадах B-мезонов

Вершинный детектор
Трековая система
Детекторы черенковских колец
Электромагнитный калориметр
Адронный калориметр
Мюонная система

Triple-GEM detectors in for inner region (R1) of the first muon station (M1)

Trigger (Level-0) and muon p_T measurements

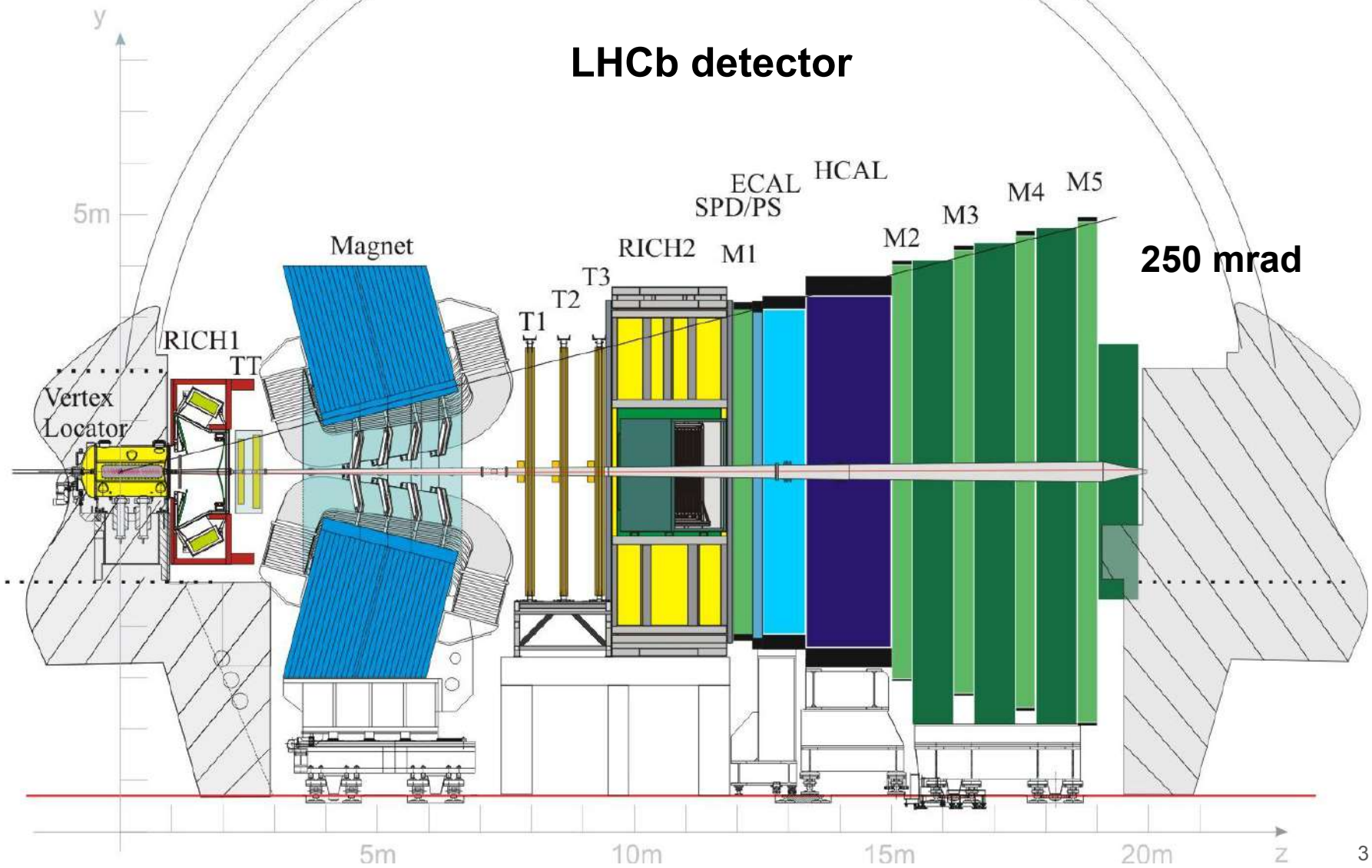

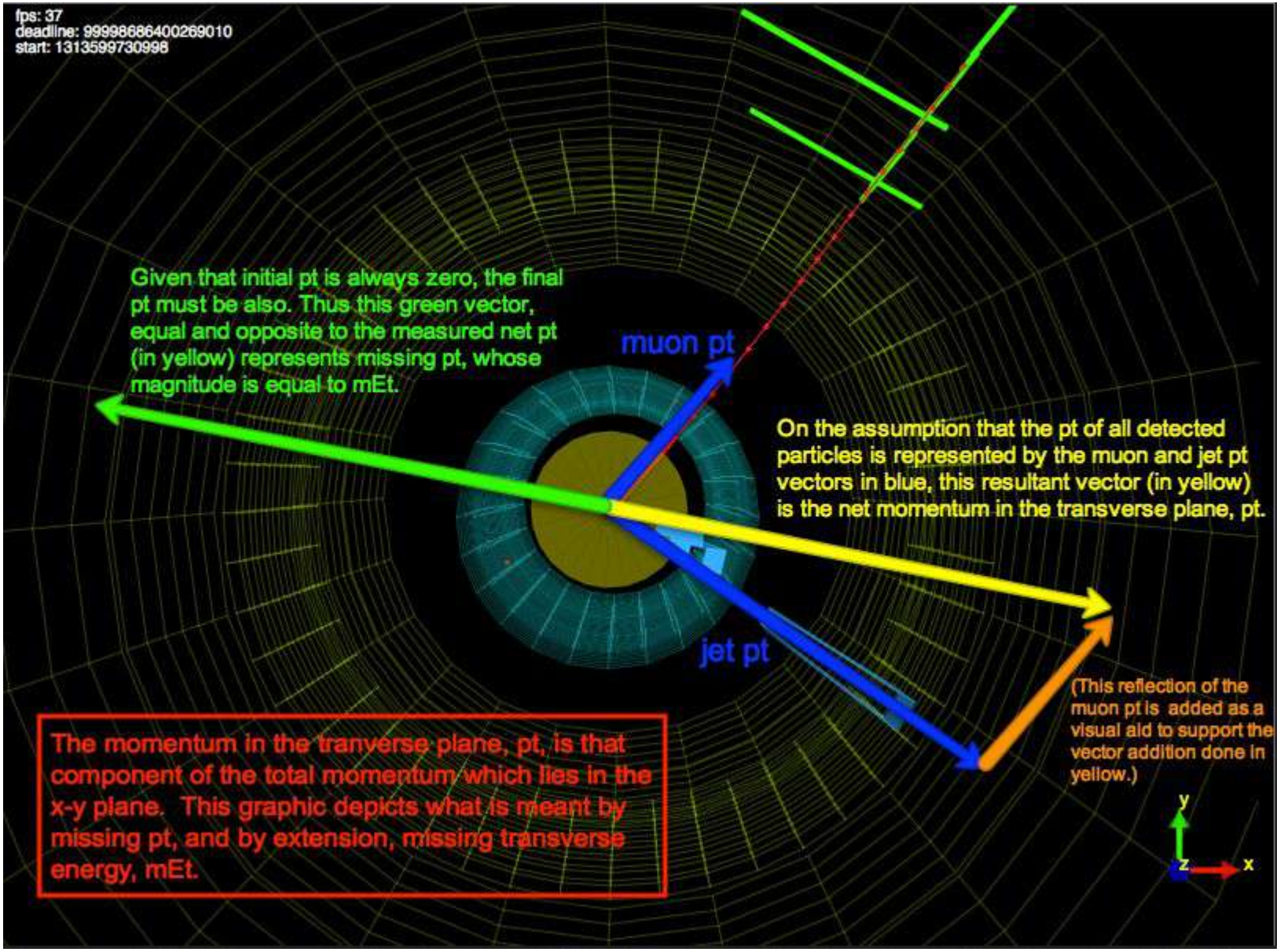
fps: 37
deadline: 9999868640026901O
start: 1313599730998
Given that initial pt is always zero, the final pt must be also. Thus this green vector, equal and opposite to the measured net pt (in yellow) represents missing pt, whose magnitude is equal to mEt.
muon pt
On the assumption that the pt of all detected particles is represented by the muon and jet pt vectors in blue, this resultant vector (in yellow) is the net momentum in the transverse plane, pt.
jet pt
(This reflection of the muon pt is added as a visual aid to support the vector addition done in yellow.)
The momentum in the tranverse plane, pt, is that component of the total momentum which lies in the x-y plane. This graphic depicts what is meant by missing pt, and by extension, missing transverse energy, mEt.
y
z
x

Università degli Studi di Roma
"Tor Vergata"

Facoltà di Scienze Matematiche, Fisiche e Naturali

Triple-GEM detectors for the innermost region of the muon apparatus at the LHCb experiment

Doctoral Thesis in Physics

Marco Poli Lener

Tutor

Dott. G. Bencivenni

Coordinator

Prof. P. Picozza

Roma 2005

B-mesons collection

	LHCb	ATLAS/CMS
Detector configuration	Single-arm forward	Central detector
Running luminosity [$cm^{-2}s^{-1}$]	2×10^{32}	3×10^{34}
pseudo-rapidity range (η)	$1.9 \div 4.9$	$-2.5 \div 2.5$
$<$ interactions/crossing $>$	$\sim$0.4 ($\sim$ 30% single int.)	$\sim$ 23
$b\bar{b}$ pairs/years(integrated in the η range)	10^{12}	5×10^{13}

Comparison of the LHC experiment parameters.

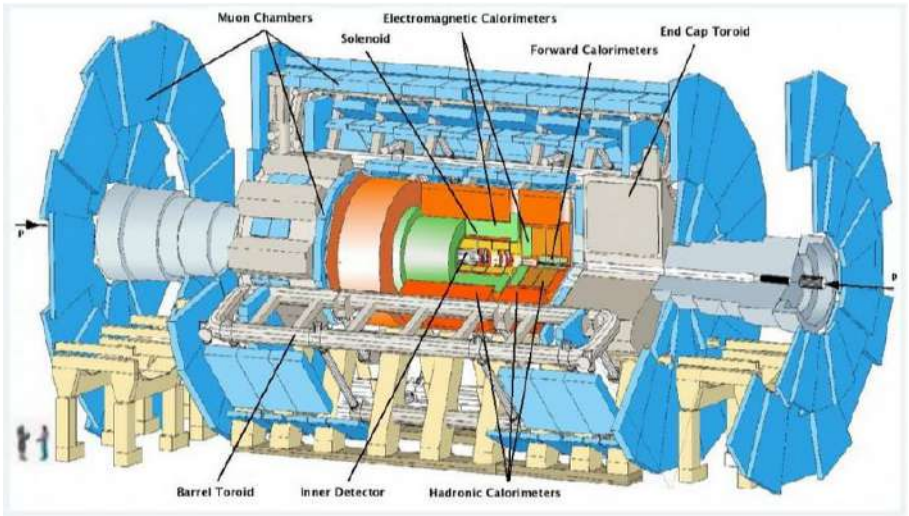

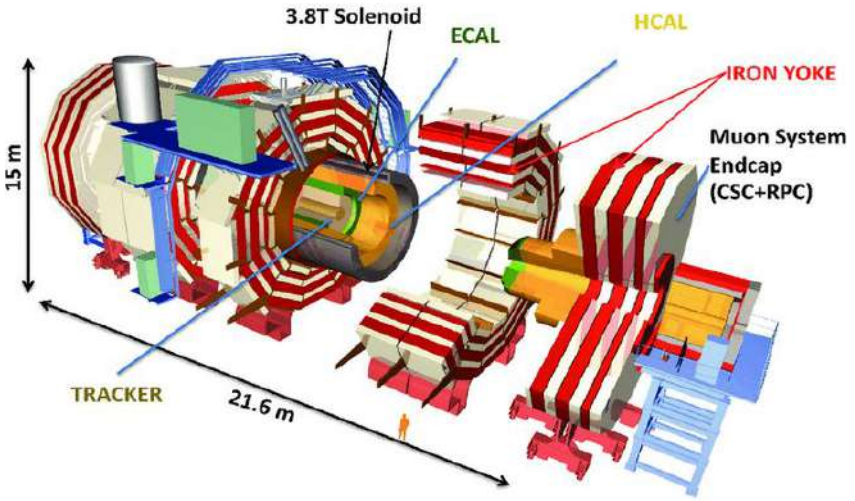

B-mesons collection

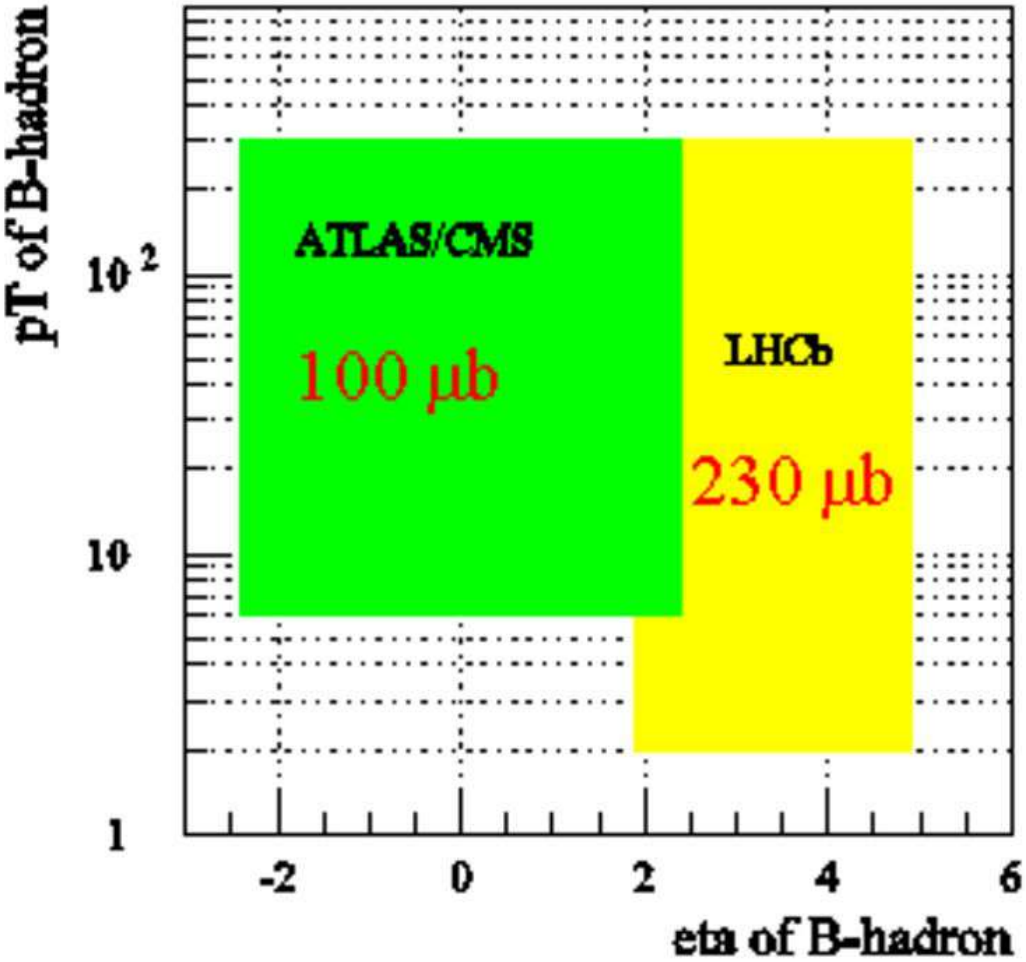

LHCb can measure B-mesons down to p_T = 2 GeV/c and has access to a visible b cross-section of about 230 µb.

ATLAS and CMS have to raise the p_T-threshold to values around 6 GeV/c in order to suppress background.

Phase space coverage of the LHC experiments for B-physics.

Trigger is very component of the LHCb experiment

Most sub-detectors designs
are motivated by triggering considerations

The bunch-crossing frequency is 40 MHz

Every 25 ns a pp event can occur

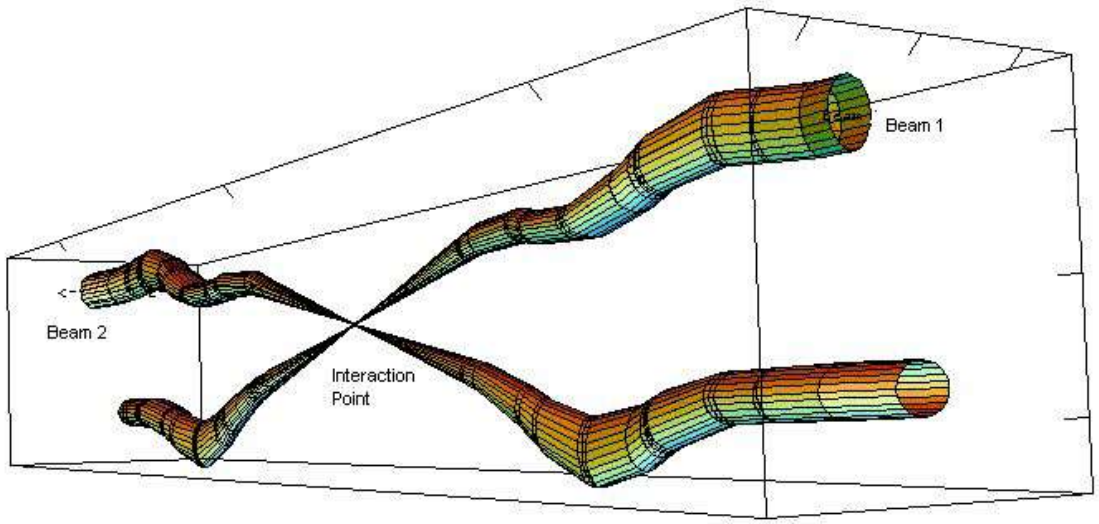

At $L = 2\times10^{32}\ cm^{-2}\ s^{-1}$
inelastic pp interaction (called minimum bias) happens **at rate 15 MHz**

Inelastic proton-proton (pp) interactions are called "minimum bias" because they represent a broad selection of events, aiming to be as unbiased as possible towards the type of interaction occurring. These events are selected by a loose trigger, which primarily includes all inelastic collisions.

The ratio of the inelastic minimum bias and bb cross-section is about 100

The bb production rate is 150 kHz

For every B event of interest there are 10^6 background events.

Level	Selects	Input rate	Reduction	Latency
Level-0	High p_T tracks	15 MHz	15	4 μs
Level-1	Secondary vertices	1 MHz	25	$\sim$ 1 ms
HLT	Reconstructed B events	40 kHz	20	
Events written on the tape		2 kHz		

Summary of the trigger scheme.

The Muon System

Muon triggering and off-line muon identification

Muons are in final states of many CP-sensitive B decays

$$B_d^0 \to J/\psi(\mu^+\mu^-)K_S^0$$

$$B_s^0 \to J/\psi(\mu^+\mu^-)\phi$$

The muon trigger is based on a muon track reconstruction and muon p_T measurement with resolution of ~ 20%

The muon detector consists of five muon tracking stations placed along the beam axis. The first station (M1) is placed in front of the calorimeter preshower, at 12.1 m from the interaction point.
Therefore, the M1 position requires a radiation length of the detector materials below 10% of X_0
The minimum momentum requested to traverse the 5 muon stations is 8 GeV/c.

The chambers within the filter are allocated about 40 cm of space
and are separated by three shields of 80 cm thickness.

The angular acceptances of the muon system is from 20 to 306 mrad in the bending plane and from 16 to 256 mrad in the non-bending plane.

This provides a geometrical acceptance of about 20% of muons from b decays relative to the full solid angle.

The total detector area is about 435 m^2.

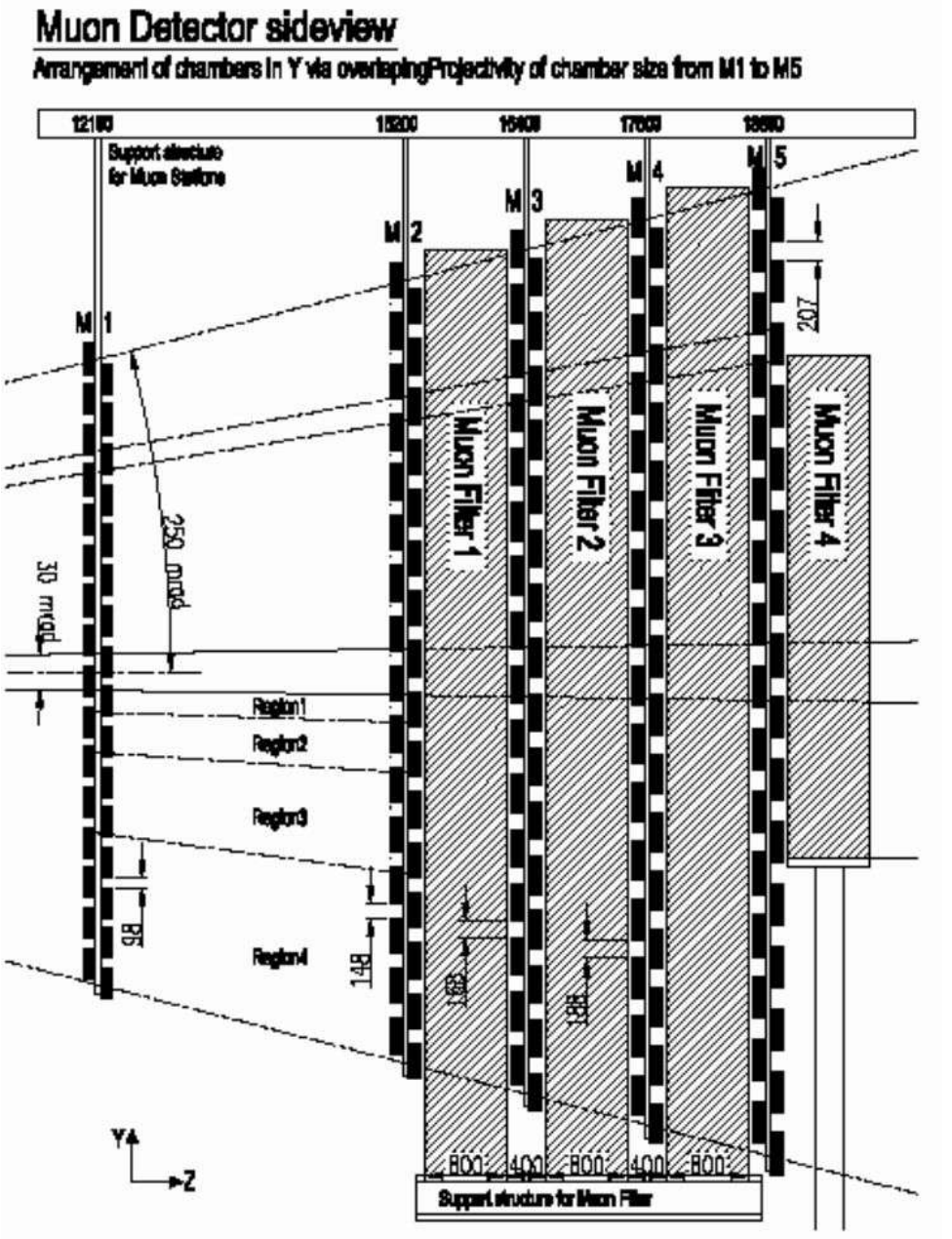

Side view of the muon system.

p_T resolution contributions

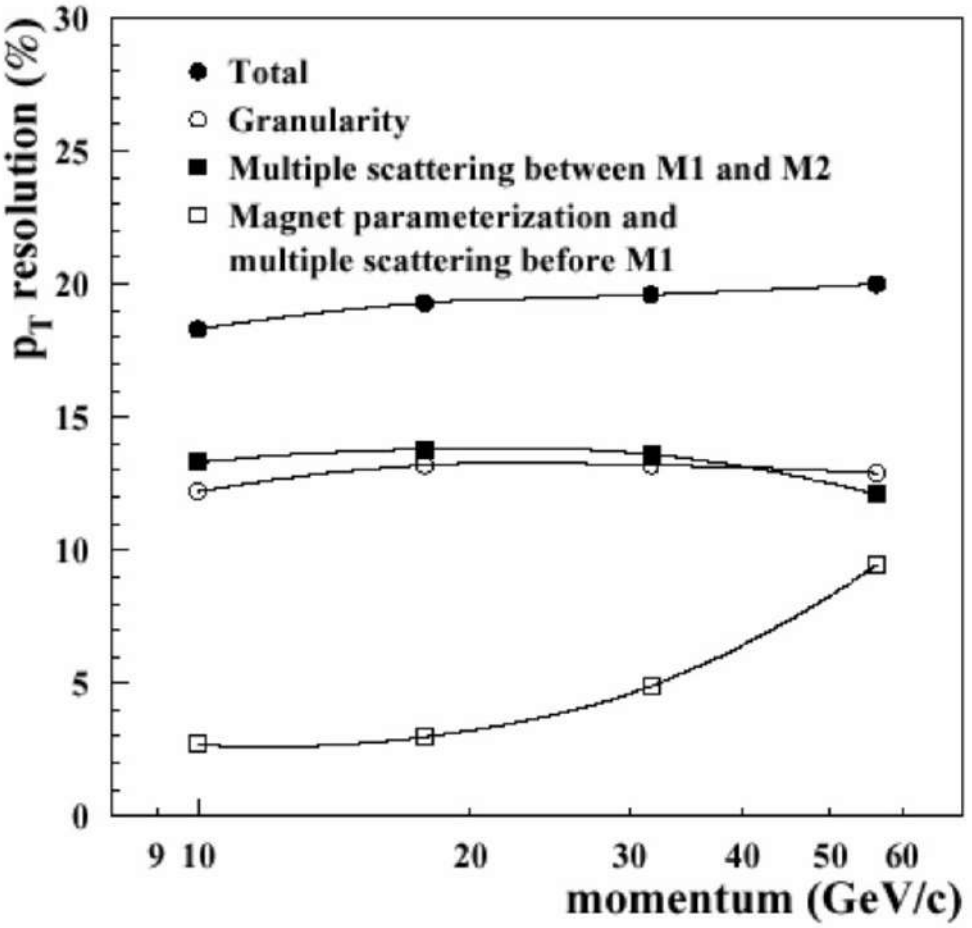

Figure 2.2: Contributions to the transverse momentum resolution of the muon system as a function of the muon momentum, averaged over the full acceptance. The p_T resolution is defined as $|p_{\mathrm{T}}^{rec} - p_{\mathrm{T}}^{true}|/p_{\mathrm{T}}^{true}$, and is shown for muons from semi-leptonic b decay having a reconstructed p_T close to the trigger threshold, between 1 and 2 GeV/c.

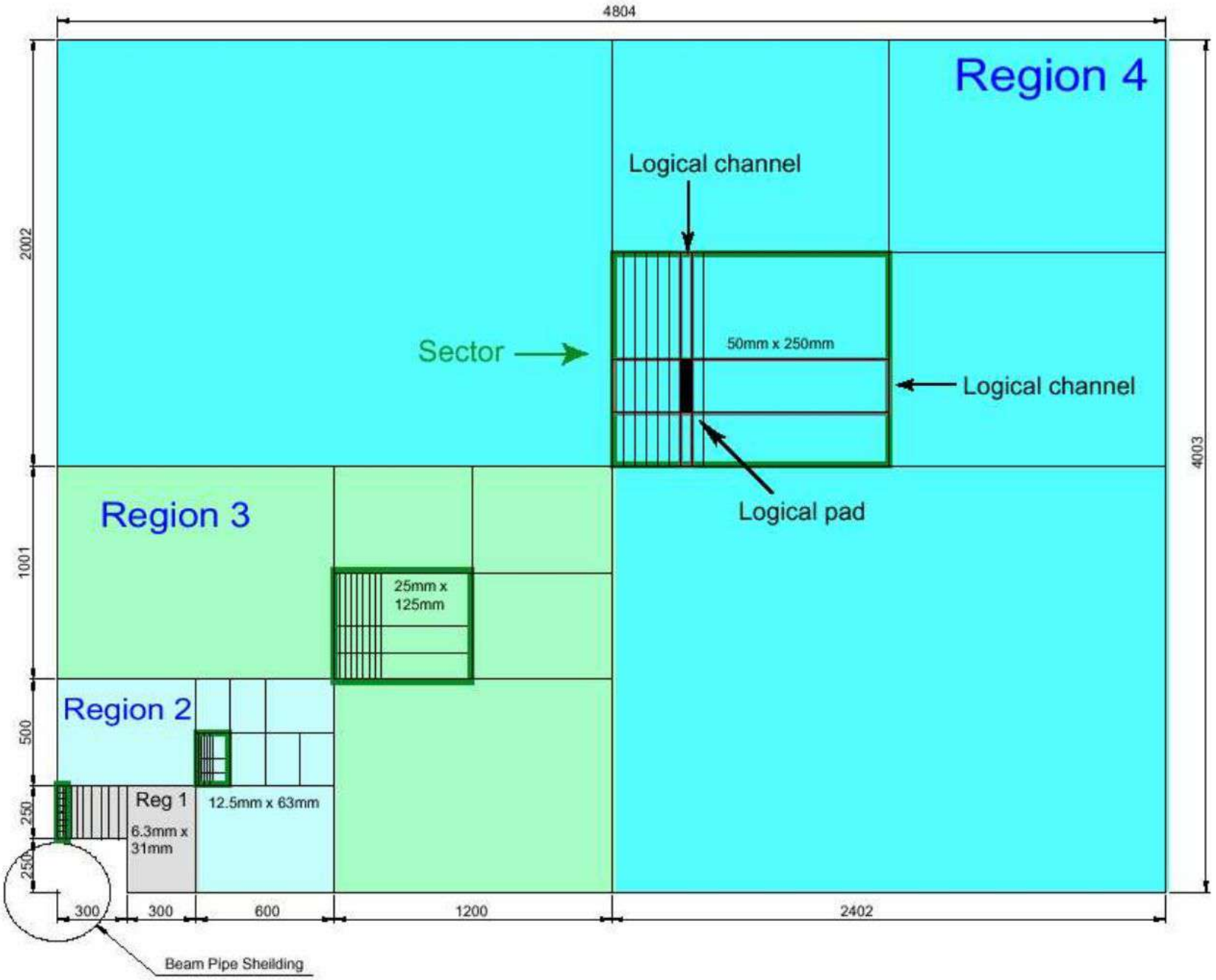
4804
Region 4
Logical channel
2002
Sector
50mm x 250mm
Logical channel
Logical pad
4003
Region 3
1001
25mm x
125mm
Region 2
500
Reg 1
12.5mm x 63mm
250
6.3mm x
31mm
250
300
300
600
1200
2402
Beam Pipe Sheilding

Each logical pad may group one or more physical pads, whose dimension are limited by occupancy and capacitance

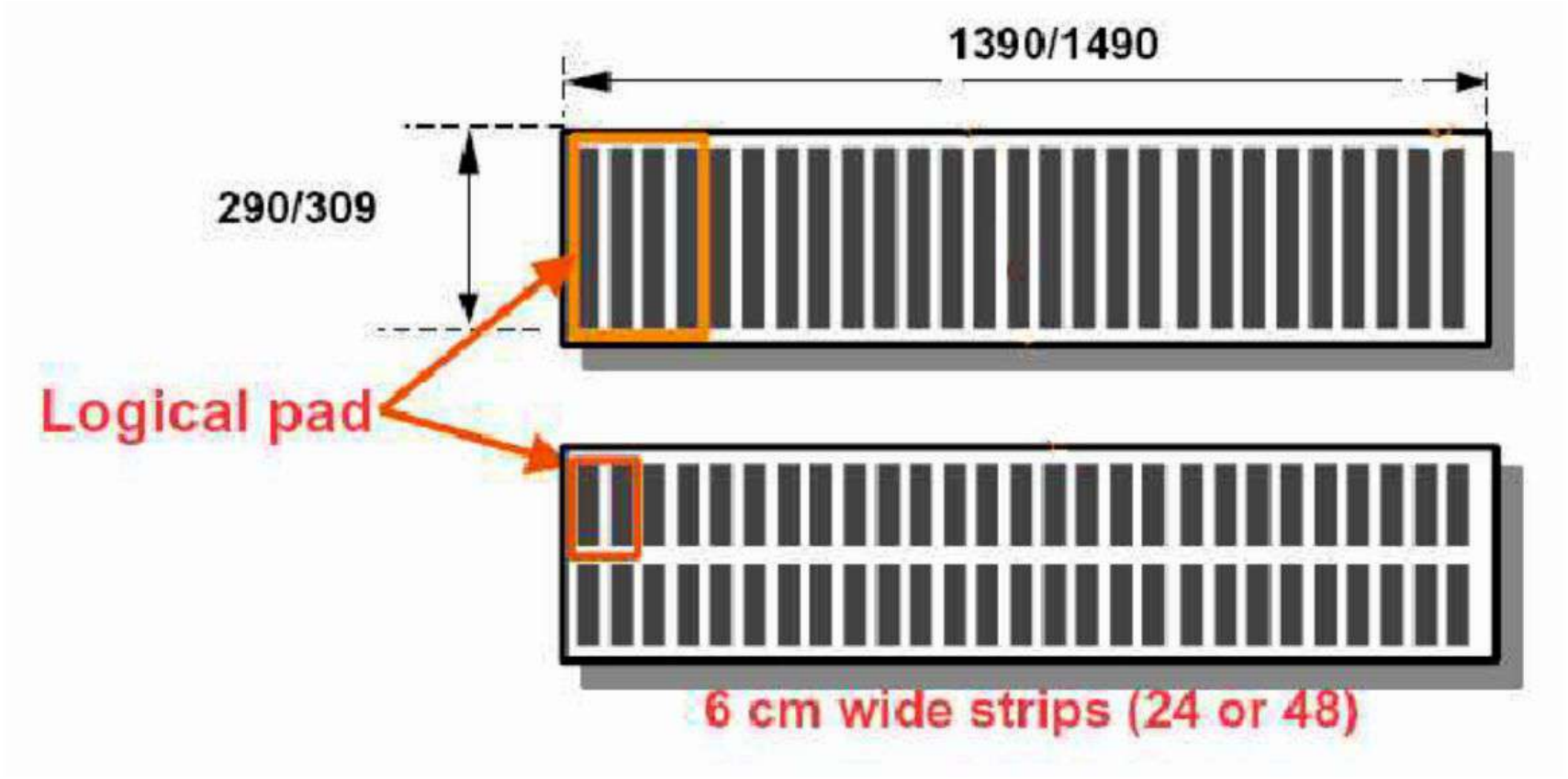

Figure 2.4: Logical pads and physical pads in Region 4 (top) and Region 2 (bottom) for Stations M4 and M5. In the former case the x dimension is that of 4 chamber strips and the y dimension is the same of the chamber itself. In the latter case more granularity is required and both x and y have half dimensions.

The basic function of the LHCb Muon system: identify and trigger muons

Fast triggering requirement

The muon Level-0 trigger (L0) is designed in such a way that information from all five muon stations is required, and looking for muon tracks with large p_T

Once track finding is completed, an evaluation of p_T is performed for muon tracks

The p_T is determined from the track hits in M1 and M2

The momentum measurement assumes a particle from the interaction point and a single kick from the magnet

Muon tracks

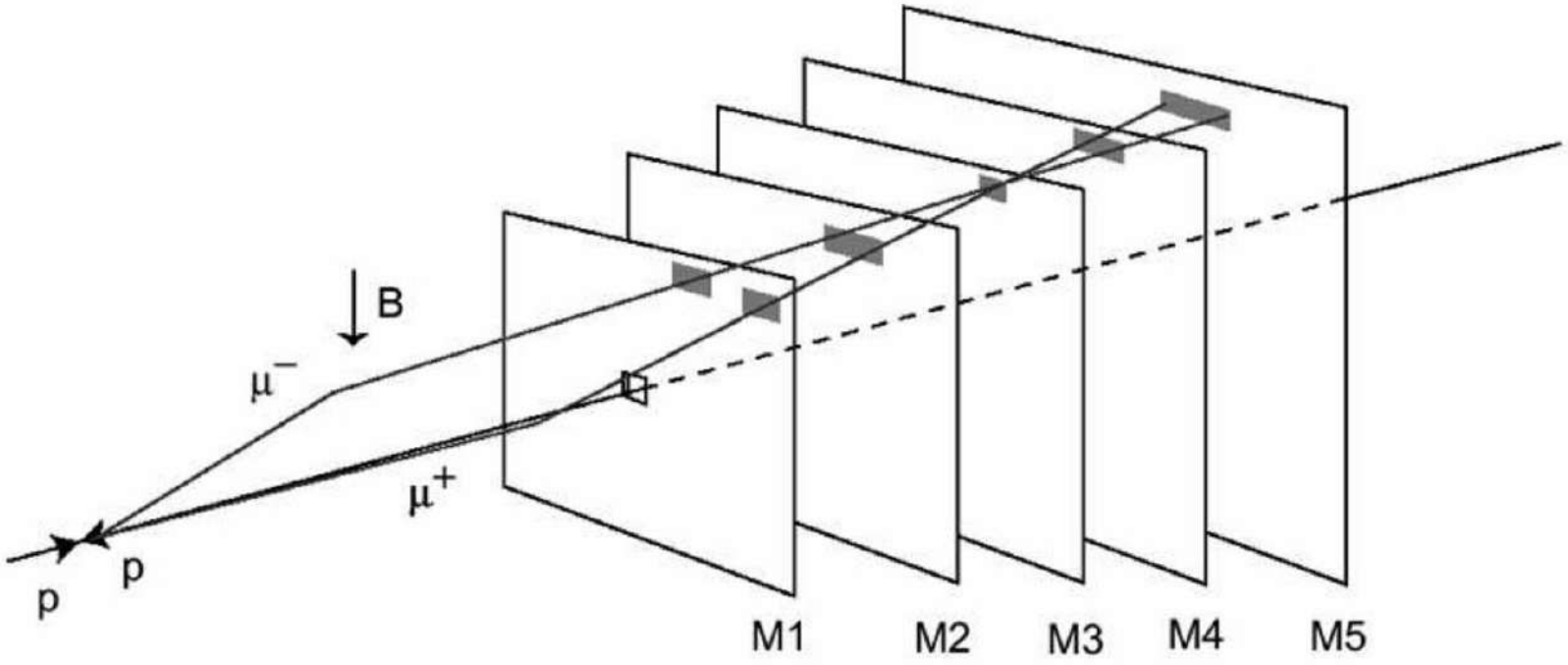

Figure 2.5: Track finding by the muon trigger. In the example shown, μ^+ and μ^- cross the same pad in M3. The highlighted in the various station represent the field of interest where the hits are searched.

Trigger efficiency

$$\epsilon_{trigger} = \left(\epsilon_{station}\right)^5$$

In order to improve the single station efficiency in 20 ns time window,
the M2-M5 stations consist of four independent detector layers, which are readout as two double layers and then logically OR-ed (логическая схема “ИЛИ”)

Only two detector layers for the M1 station
in order to reduce material budget in front of the calorimeters

The **efficiency for M2-M5 stations must be > 99%**,
and **> 96% for the M1 station**, where only two detector layers are foreseen

As result of such stations efficiency requirement,
the **L0 trigger efficiency** comes out to be **higher than 92%**

Background environment

	Station 1	Station 2	Station 3	Station 4	Station 5
Region 1	230 kHz/cm^2 460 kHz/cm^2	7.5 kHz/cm^2 37.5 kHz/cm^2	2 kHz/cm^2 10 kHz/cm^2	2.3 kHz/cm^2 6.5 kHz/cm^2	880 kHz/cm^2 4.4 kHz/cm^2
Region 2	93 kHz/cm^2 186 kHz/cm^2	5.3 kHz/cm^2 26.5 kHz/cm^2	650 Hz/cm^2 3.3 kHz/cm^2	430 Hz/cm^2 2.2 kHz/cm^2	350 Hz/cm^2 1.8 kHz/cm^2
Region 3	40 kHz/cm^2 80 kHz/cm^2	1.3 kHz/cm^2 6.5 kHz/cm^2	200 Hz/cm^2 1.0 kHz/cm^2	150 Hz/cm^2 750 Hz/cm^2	130 Hz/cm^2 650 Hz/cm^2
Region 4	12.5 kHz/cm^2 25 kHz/cm^2	230 Hz/cm^2 1.2 kHz/cm^2	83 Hz/cm^2 415 Hz/cm^2	50 Hz/cm^2 250 Hz/cm^2	45 Hz/cm^2 225 Hz/cm^2

Table 2.1: Particle rates in the muon system.The first row gives the calculated rate at a luminosity of $\mathcal{L} = 5\times10^{32}$ cm^{-2} s^{-1} assuming a total $p-p$ cross-section of σ=102.4 mb; in the second row the rate includes the safety factors.

Muon system detector technologies

The combination of physics goals and background conditions have determined the choice of detector technologies for the various stations and regions.
The following **parameters** particularly **affects the technology choice**:
1. Rate capability: The selected technologies must tolerate the expected particle rate without efficiency losses;
2. Ageing: The detector must tolerate, without damages or performance losses, the integrated charge accumulated in 10 years of operation;
3. Time resolution: The muon system must provide unambiguous bunch crossing identification with high efficiency. The requirement is at least 99% efficiency within 20 ns window for M2-M5 stations.
For M1 station, as previously discussed, this efficiency is less stringent (> 96%);
4. Spatial resolution: A good spatial resolution is required, especially in M1 and M2, in order to obtain an accurate p_T evaluation (~20%)

Based on the above considerations, the ~ **99% of the area of the Muon system** will be equipped with **Multi Wire Proportional Chamber (MWPC)**

The **innermost region (R1) of the first station (M1)**,
where a particle flux up to ~ **500 kHz/cm^2** is expected, will be instrumented with **triple-GEM detectors (Gas Electron Multiplier)**

It should be stressed that the **M1R1 region, of about ~ 0.6 m^2 area**,
will **trigger about 20% of the muons**

Rate capability (загрузочная способность)

MWPC : below **1 MHz/cm^2**

GEM : up to **100 MHz/cm^2**

The use of triple-GEM detector as a triggering device was a novelty (2005) in the field of high energy physics.

The first application of GEM detectors in high energy physics was the COMPASS experiment, where triple-GEM used as a tracking device

The optimization of the time performance

Time resolution with an **Ar/CO_2 (70/30)** gas mixture is about **10 ns** r.m.s
Task: improve this limit

Газовый электронный умножитель был изобретён Фабио Саули в 1996 году

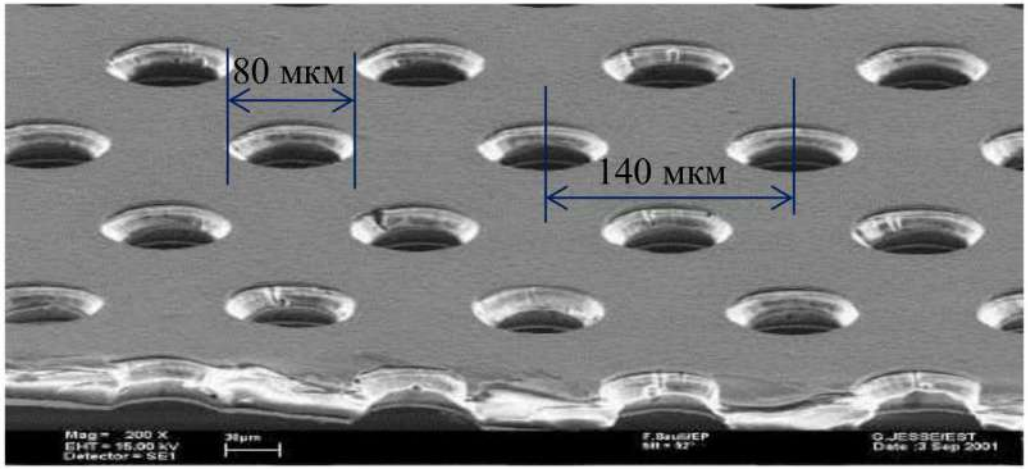

Изображение ГЭУ, полученное на сканирующем электронном микроскопе

Диэлектрическая каптоновая плёнка толщиной 50 мкм, покрытая с двух сторон медью толщиной 5 мкм

Отверстия имеют форму двойного конуса

F. Sauli, GEM: A new concept for electron amplification in gas detectors // Nucl. Instrum. and Methods. A386 (1997) 531

Изготовление ГЭУ

ГЭУ изготавливаются
с помощью фотолитографии
путём химического травления
металла и диэлектрика
с обеих сторон

50 мкм каптона и 5 мкм
меди с обеих сторон

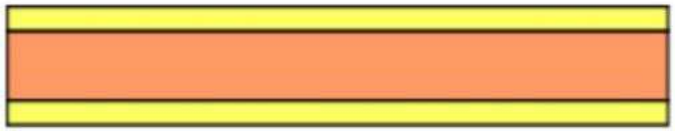

Нанесение фоторезиста и
фотошаблона, освещение
ультрафиолетом

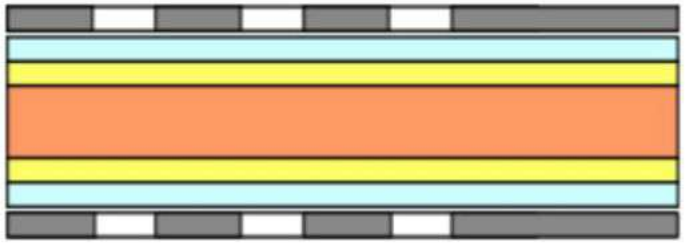

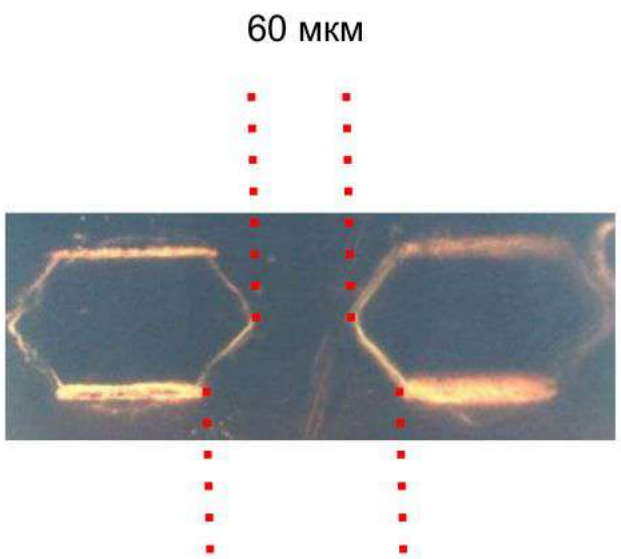

Травление
металла

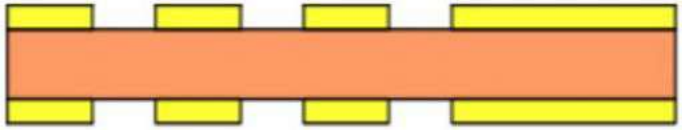

Травление
каптона

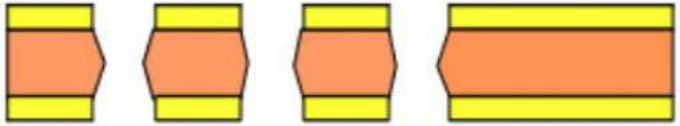

Принцип действия ГЭУ

Медь на каптоне - это электроды, на которые подаётся напряжение.

Силовые линии поля фокусируются в отверстия

Напряжённость в центре отверстия ~50 кВ/см

Детектируемые частицы
производят ионизацию в рабочем газе

Первичные электроны ионизации дрейфуют вдоль силовых линий и фокусируются в отверстия, в которых под действием сильного электрического поля развиваются электронные лавины

Часть электронов лавины может выйти из отверстия в газовый промежуток для усиления в последующих усилительных каскадах или для регистрации на анодном (считывающем) электроде

Способность ГЭУ работать в каскадной конфигурации является его главным преимуществом перед другими газовыми детекторами

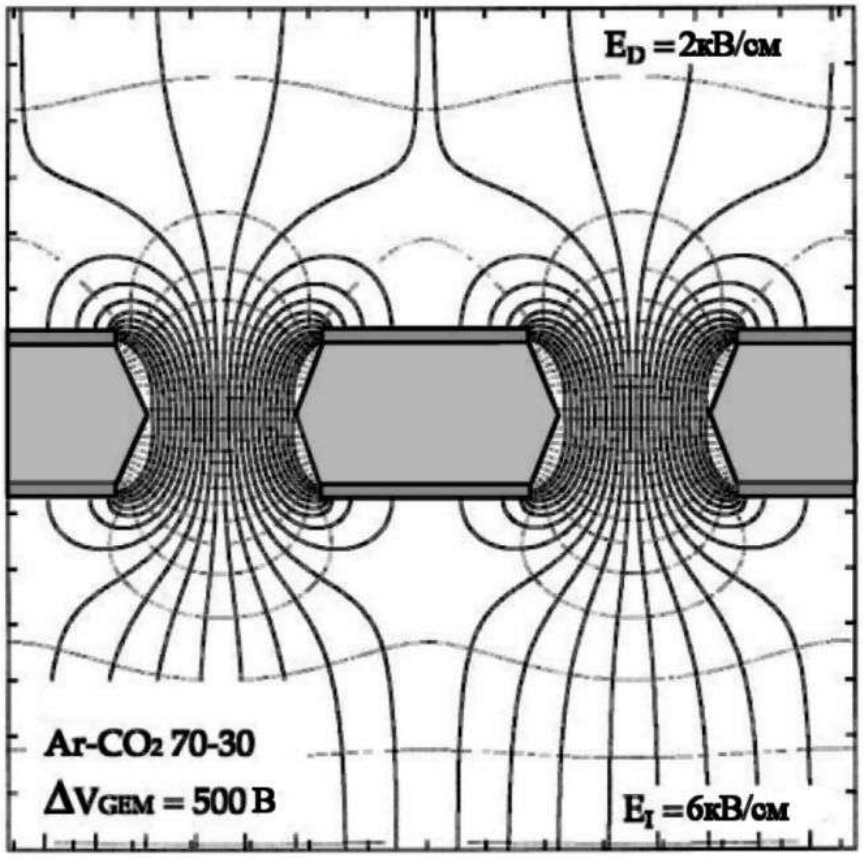

Картина электрического поля в ГЭУ
для типичных условий работы

Bachmann S., Bressan A., Ropelewski L. et al.
Charge amplification and transfer processes in the gas electron multiplier
// Nucl. Instrum. and Methods. 1999. Vol. A438.

Принцип действия ГЭУ

Некоторые силовые линии замыкаются на нижнем электроде ГЭУ

Поэтому значительная часть электронов лавины будет собираться на нём и будет потеряна для регистрации на считывающем электроде

Реальное усиление ГЭУ соответствует полному заряду в лавине

Эффективное усиление соответствует заряду, измеряемому на считывающем электроде

Эффективное усиление всегда меньше реального

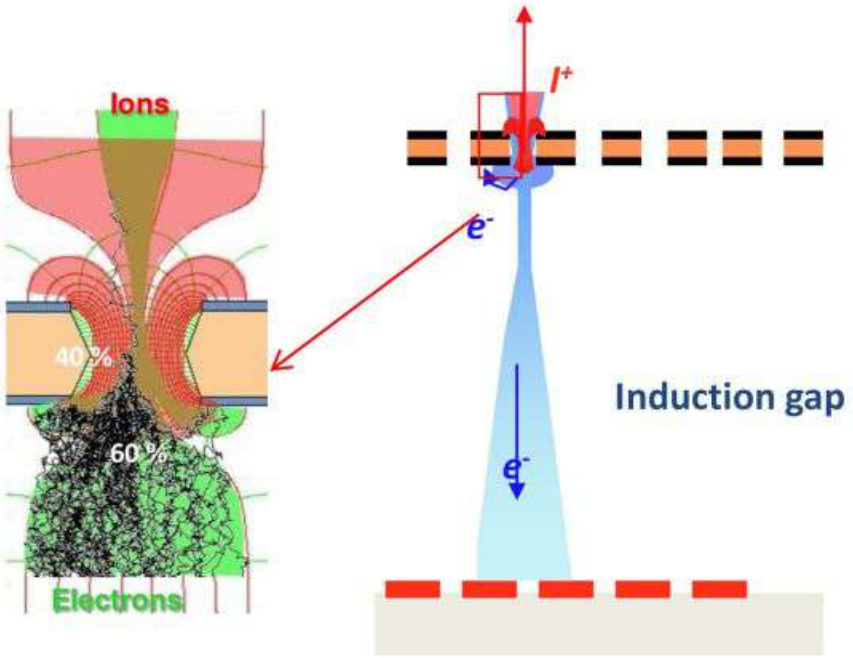

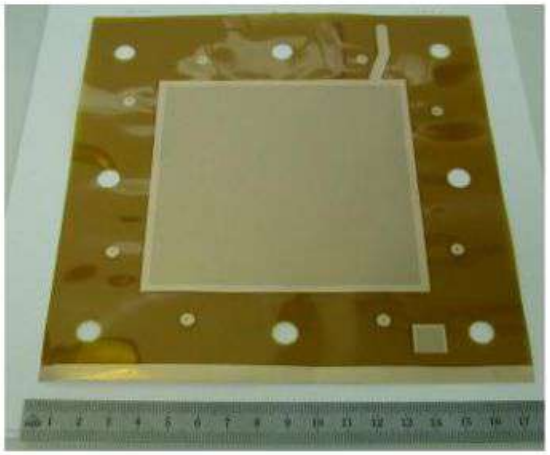

Внешний вид ГЭУ

Виды считывающих структур

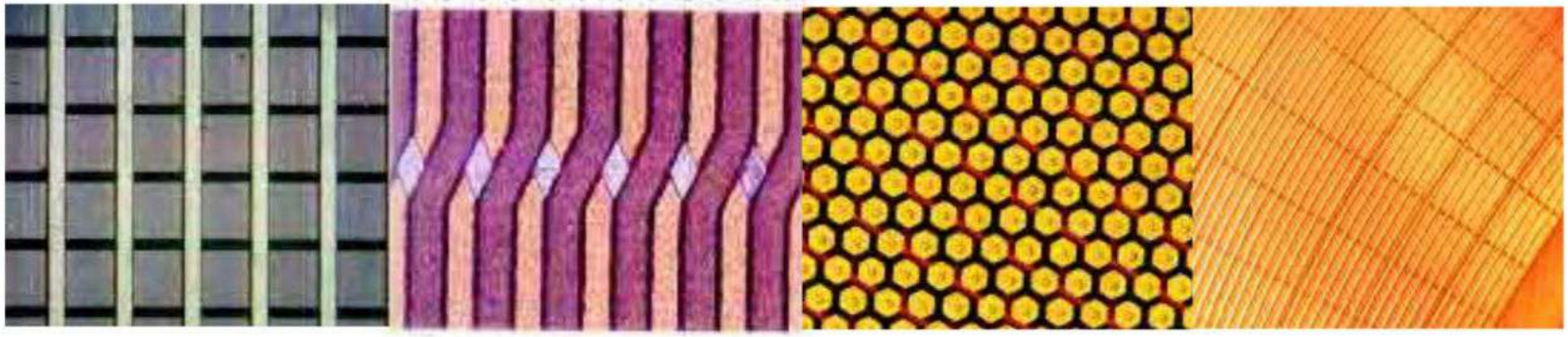

cartesian | small angle | hexaboard | strips-on-pads

COMPASS, LHCb

MICE (Muon Ionization Cooling Experiment)

TOTEM

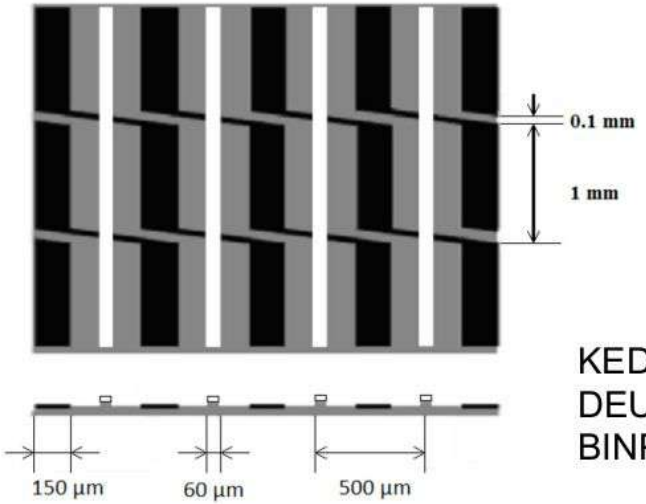

KEDR Tagging System,
DEUTERON,
BINP

TBF, BINP

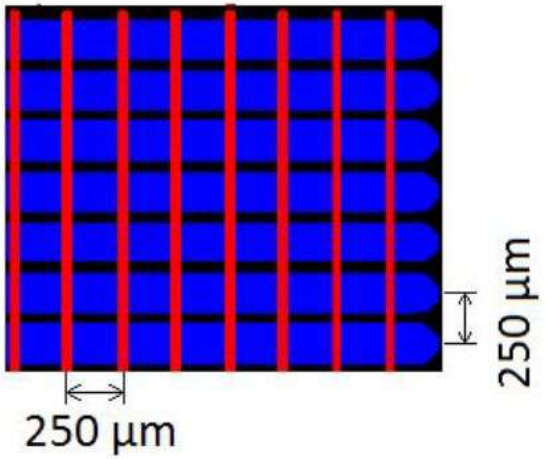

Triple-GEM detector

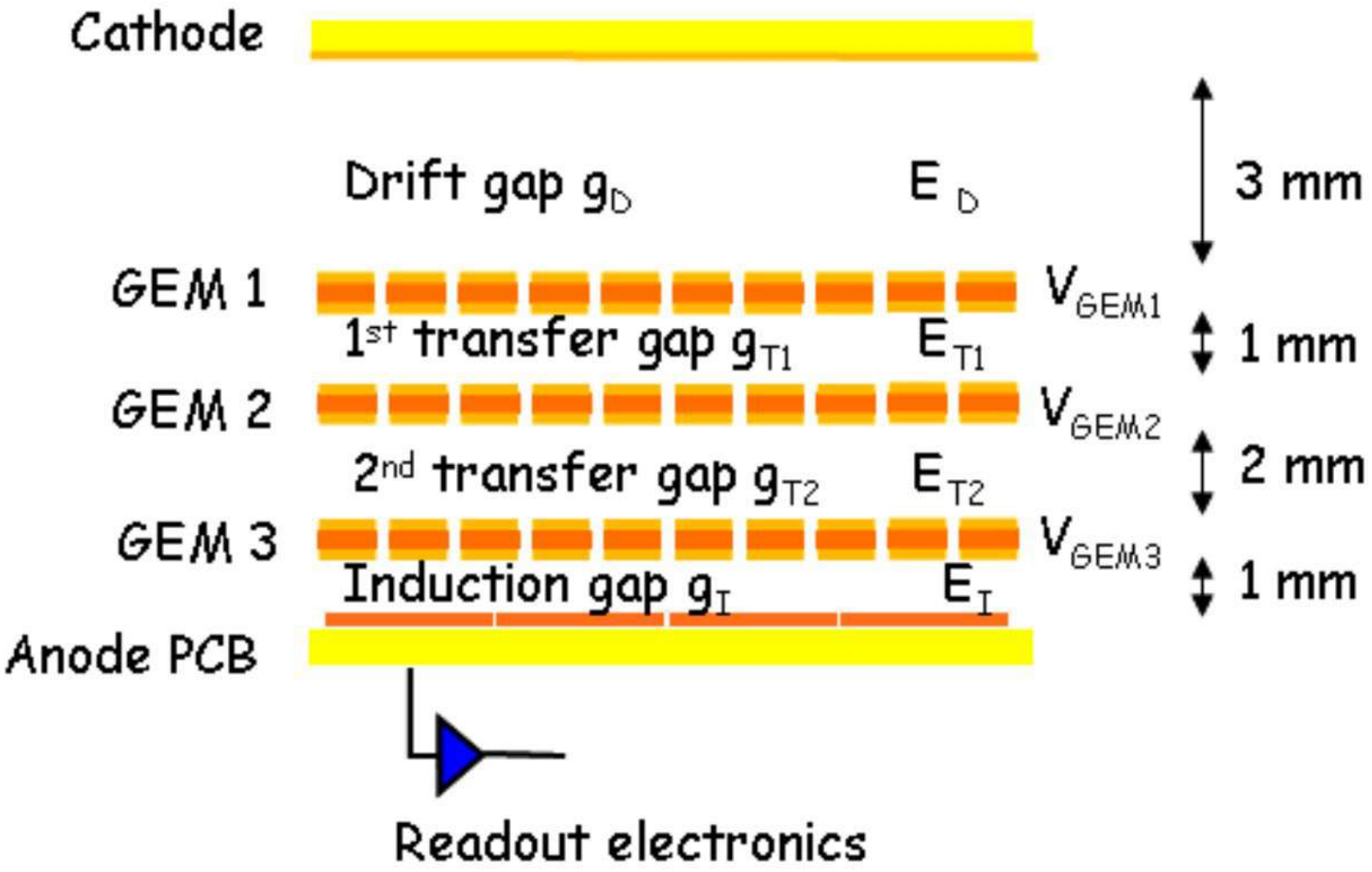

Discharge probability as a function of the gas gain
for a single, double and triple-GEM detectors in Ar/CO_2 (70/30) gas mixture

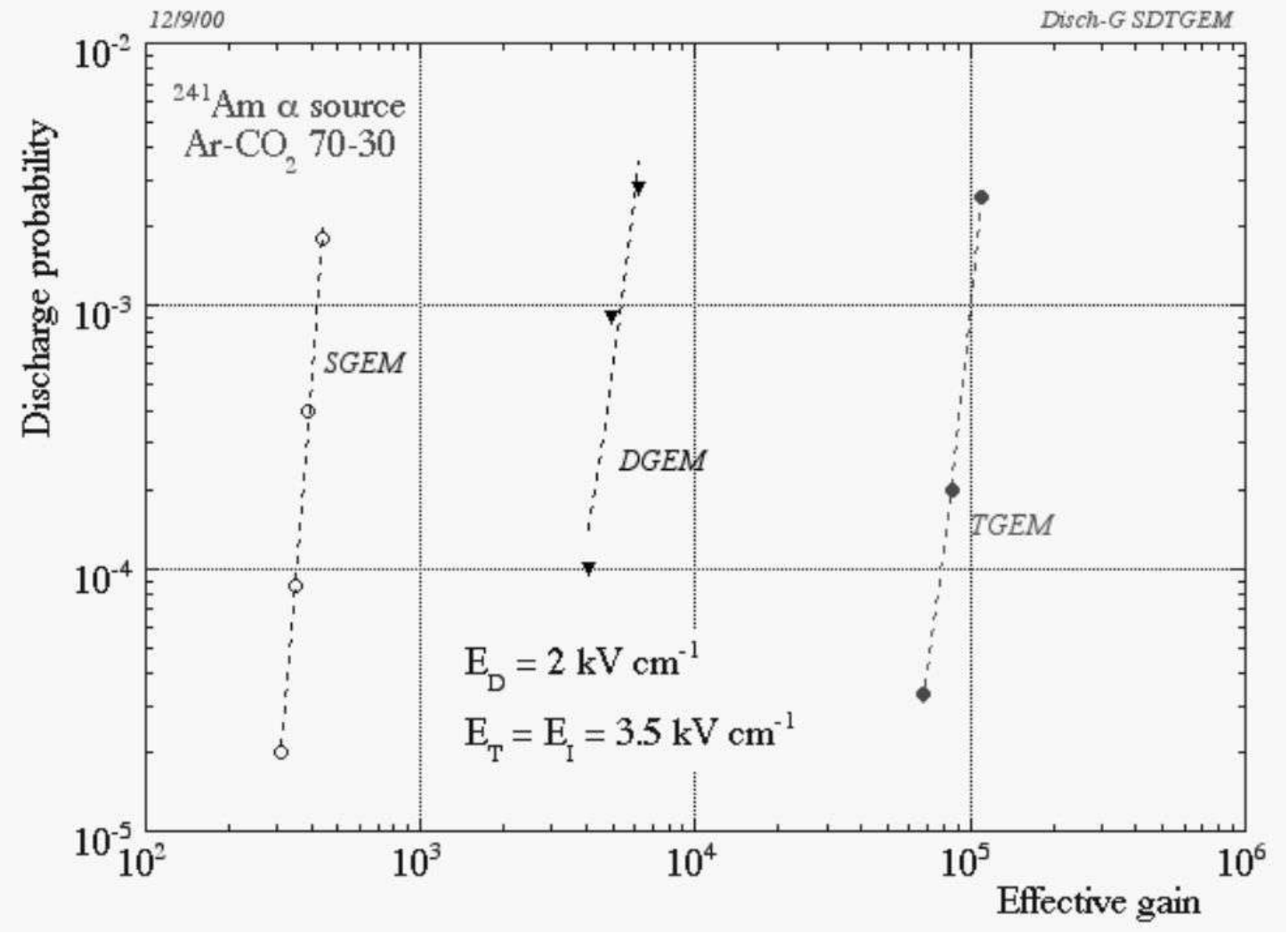

Due to statistical fluctuations of the total ionization and the gas gain, **the ionization produced in the first transfer gap**, and multiplied by the last two GEMs, **can induce a signal large enough** to be read by the front-end electronics.

This effect, particularly important for the time performance of the detector, has been called bi-GEM effect

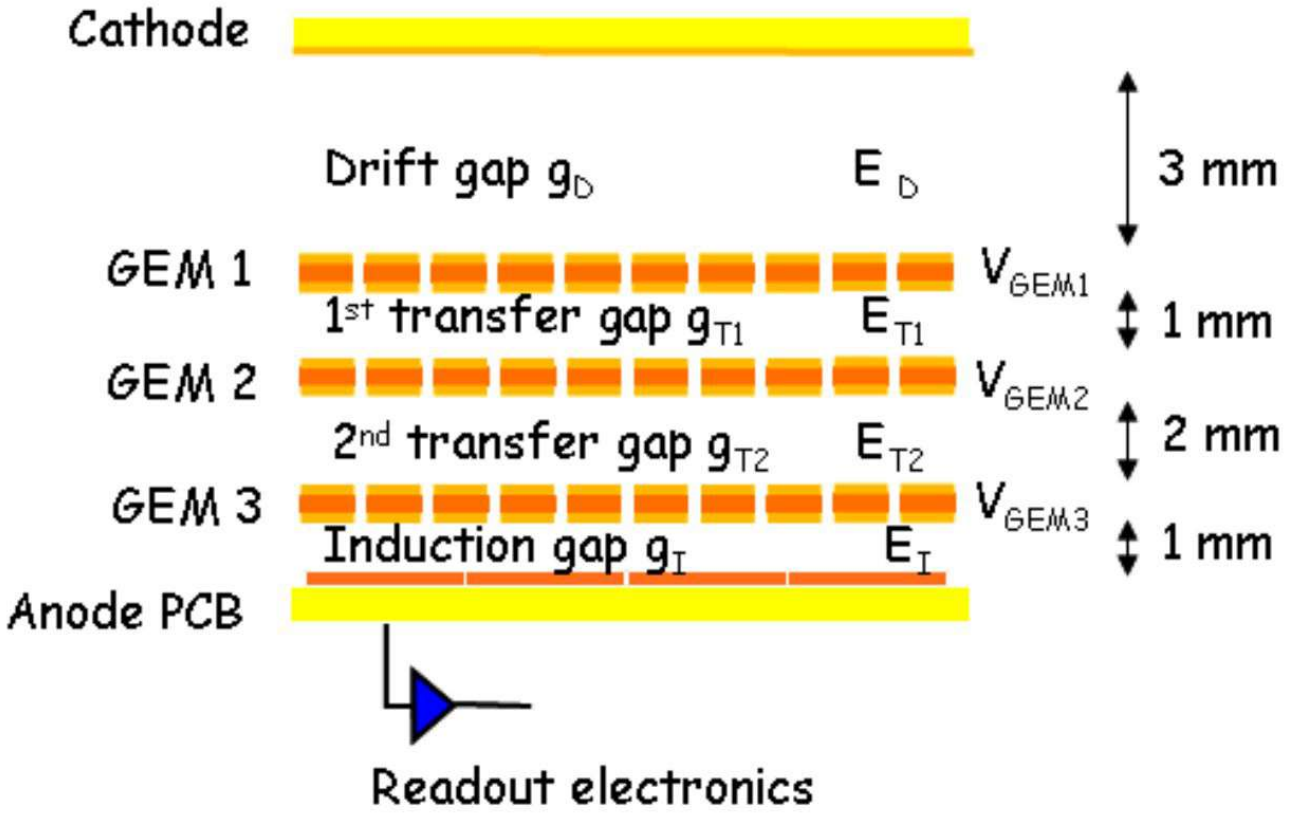

The bi-GEM signal for a triple-GEM detector (recorded in common stop):
time spectrum for 1 mm (red) and 2 mm (black) thickness of the first transfer gap

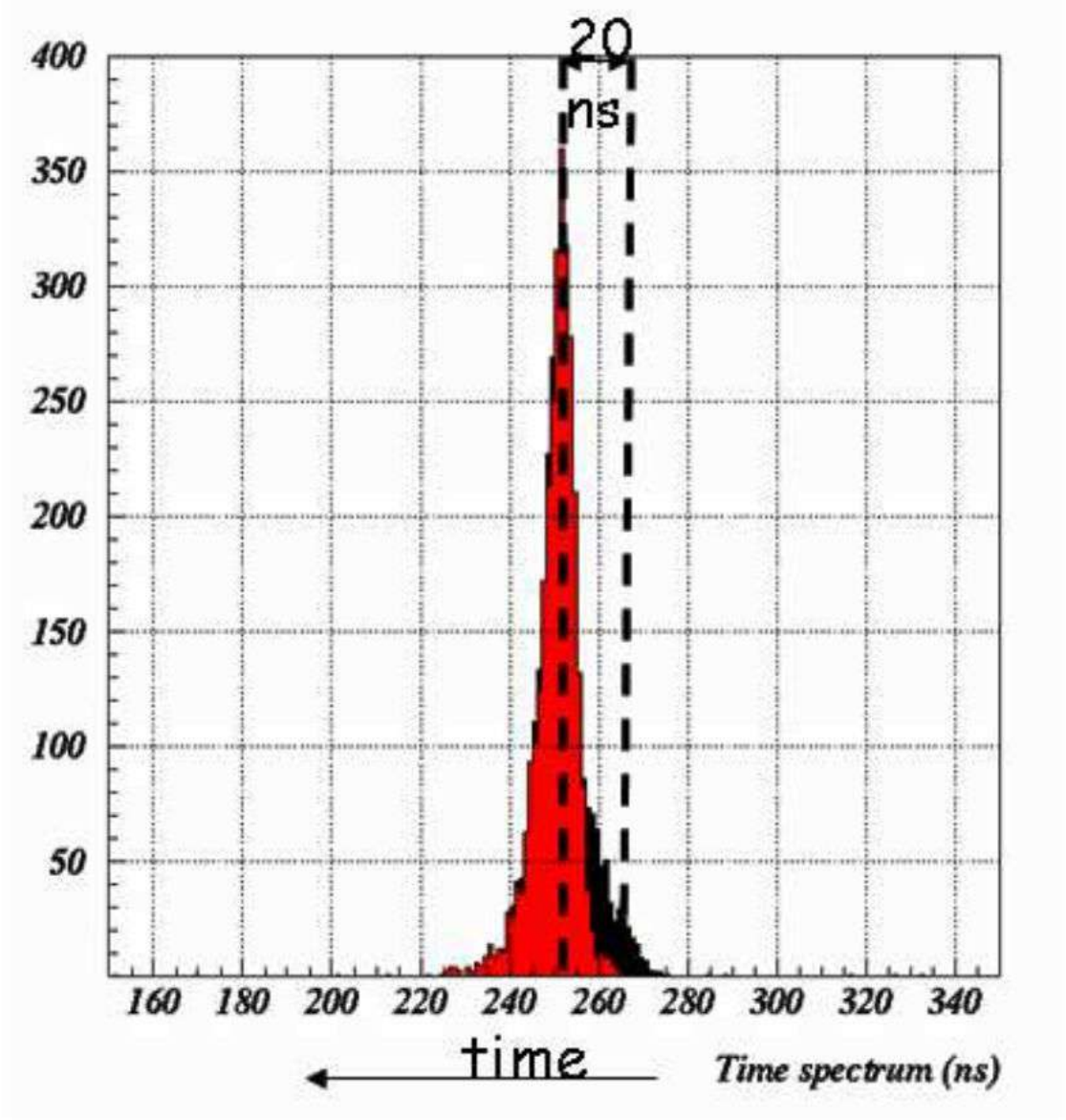

For all gas detectors, the discharge effect can be minimized by adding a suitable fraction of a quencher component to the gas mixture, although the quantity and the type are limited by the degradation of the detector performance due to ageing processes

For a triple-GEM detector using a given gas mixture,
the discharge effect can be reduced by increasing the thickness of the second transfer gap.
Indeed, a larger gap allows to increase the electron diffusion in that region.
Since the transverse dimension of the electron clouds increases with the square root of the electron drift, the number of the holes involved in the multiplication process increase linearly with the thickness of a gap. Consequently, the diffusion allows the electron cloud to be spread over more than a single hole, reducing the probability of reaching the Raether limit in the third GEM

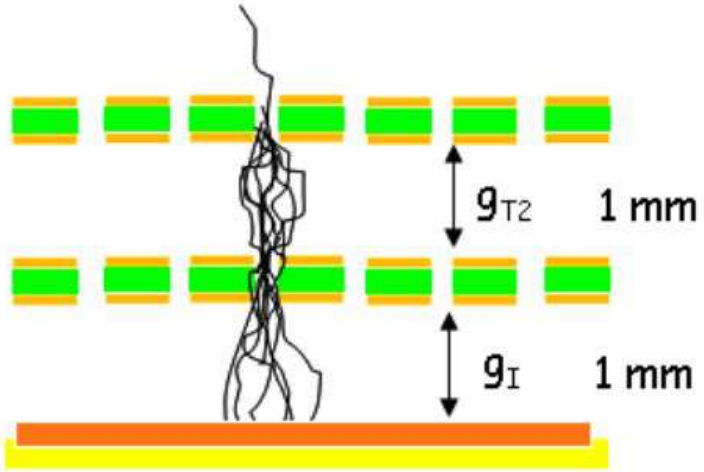

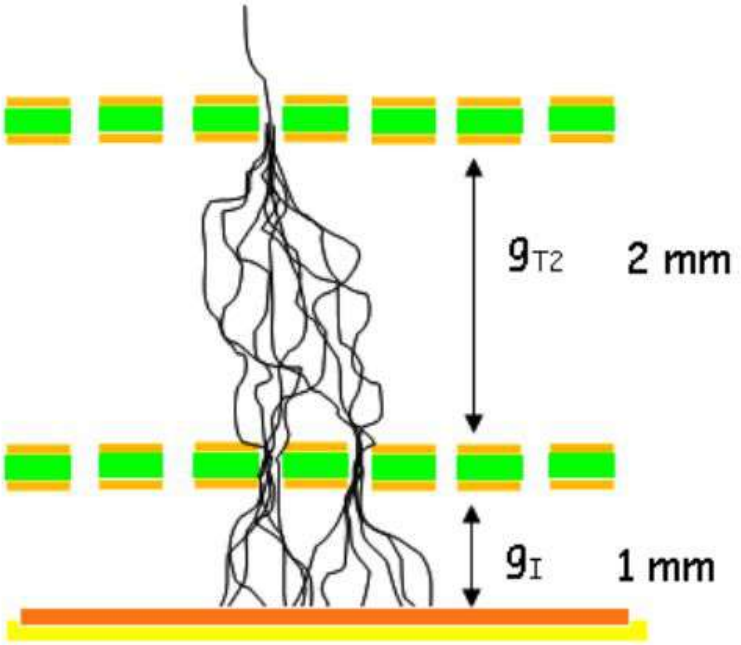

The measure of the **discharge probability**,
as a function of the gas gain in the $Ar/C0_2/CF_4$ (60/20/20) gas mixtures,
for two different thickness of the second transfer gap, 1 mm and 2 mm
respectively, has been performed with an ^{241}Am (α) source

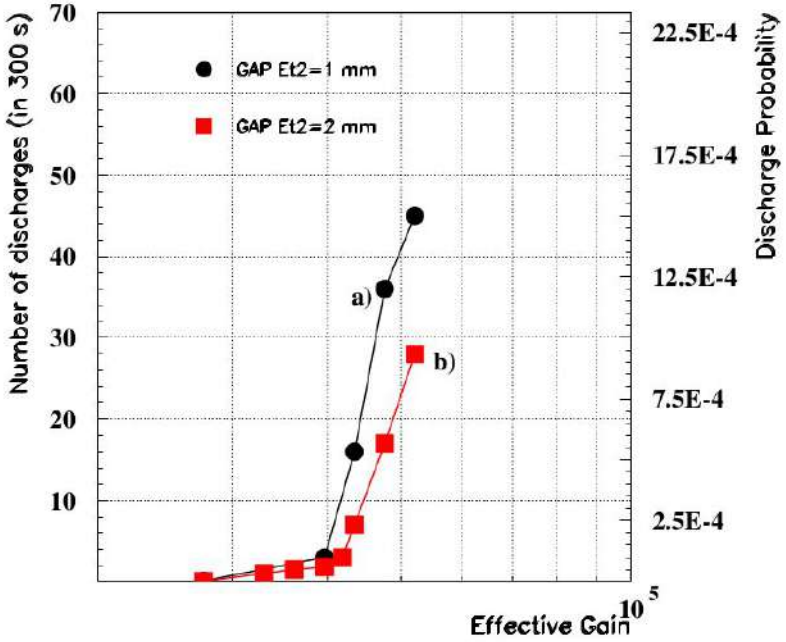

Figure 3.22: The discharge probability, performed with an ^{241}Am source, as a function of the gas gain in the $Ar/C0_2/CF_4$ (60/20/20) gas mixtures for 2 different thickness of the second transfer gap, 1 and 2 mm.

Taking into account
the maximum size required
by the muon system for the
whole detector thickness
and at the same time
the necessity to minimize
the discharge effect,
transfer gap 2 mm
was set

For a triple-GEM detector the intrinsic **gain is an exponential function** of total voltage on the GEMs

$$G_{eff} = G_{intr} \cdot T_{tot} = \prod_{k=1}^{3} e^{<\alpha>_k \cdot V_{GEMk}} \cdot T_k = e^{<\alpha>^{tot} \cdot V_{GEM}^{tot}} \cdot \prod_{k=1}^{3} \epsilon_k^{coll} \cdot f_k^{extr}$$

The **optimal configuration** of the GEM voltages is

$$V_{GEM1} \gg V_{GEM2} \geq V_{GEM3}$$

This GEM voltage configuration, reducing the discharge effect, allows also to improve the detector time performance due to a decrease of the bi-GEM effect

The above GEM voltage configuration, together with 1 mm thick first transfer gap, allow to reduce the bi-GEM down to 1%

Time performance

The main request for triggering in LHCb Muon system:
provide a high efficiency in the bunch crossing time window

The time performance of a GEM-based detector is correlated with the statistics of the cluster in the drift gap.

The general expression for the space-distribution of the cluster j created at distance x from the first GEM, is :

$$A_j^{\overline{n}}(x) = \frac{x^{j-1}}{(j-1)!}\overline{n}^j e^{-\overline{n}x}$$

where $\overline{n}$ is the average number of clusters created per unit length. For a given drift velocity in the drift gap, v_d, the probability-distribution of the arrival times on the first GEM for the cluster j gives:

$$P_j(t_d) = A_j^{\overline{n}}(v_d t_d)$$

Specifically for the first cluster produced closest to the first GEM ($j = 1$):

$$P_1(t_d) = \overline{n} \cdot e^{-\overline{n} v_d t_d} \quad \Rightarrow \quad \sigma_1(t_d) = \frac{1}{\overline{n} \cdot v_d}$$

The latter gives the *intrinsic* value for the time resolution of the detector if the first cluster is always detected.

Time performance

A **high primary ionization and a fast gas mixture**
should be chosen in order **to improve the time performance** of a GEM detector.

Simulation study of the gas mixture properties has been done by using the following **simulation tools**:

• Magboltz, which computes the electron drift velocity, the longitudinal and the transverse diffusion coefficients;
• Heed, which calculates the energy loss through the ionization of a particle crossing the gas and allows to simulate the cluster production process;
• Imonte, which computes the Townsend and attachment coefficients;

The intrinsic time resolution, which depends on the inverse of the product of the drift velocity and the specific primary ionization in the drift gap had been evaluated using Magboltz and Heed simulation tools

Simulated electron drift velocity for the studied gas mixtures

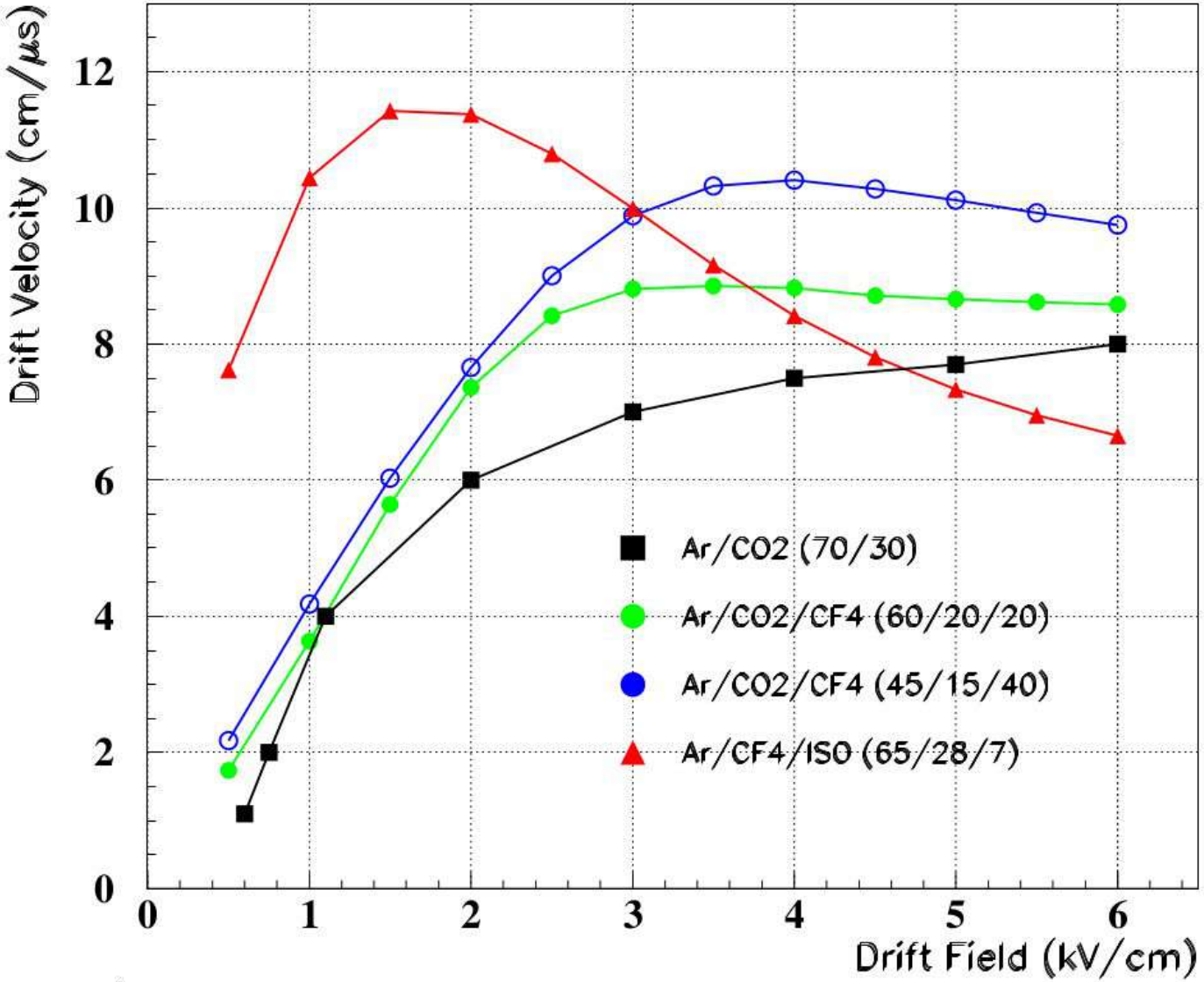

$$10\ \frac{cm}{\mu s} = 10\ \frac{10^4\ \mu m}{10^3\ ns} = 100\ \frac{\mu m}{ns} = 0.1\ \frac{mm}{ns}$$

Gas mixture properties in the simulation

Gas Mixture	Drift velocity (drift field)	< Clusters/mm >	Intrinsic time resolution
Ar/CO_2 (70/30)	7 cm/μs (@3 kV/cm)	3.3	4.7 ns (@3 kV/cm)
$Ar/CO_2/CF_4$ (60/20/20)	9 cm/μs (@3 kV/cm)	5	2.3 ns (@3 kV/cm)
$Ar/CO_2/CF_4$ (45/15/40)	10.5cm/μs (@3.5 kV/cm)	5.5	1.7 ns (@3.5 kV/cm)
Ar/CF_4/iso-C_4H_{10} (65/28/7)	11.5 cm/μs (@2kV/cm)	5.7	1.5 ns (@2 kV/cm)

Table 3.1: Summary table of the gas mixture properties: optimized drift velocity and average cluster yield. The relative *intrinsic* time resolution is also reported.

Intrinsic time resolution in the simulation

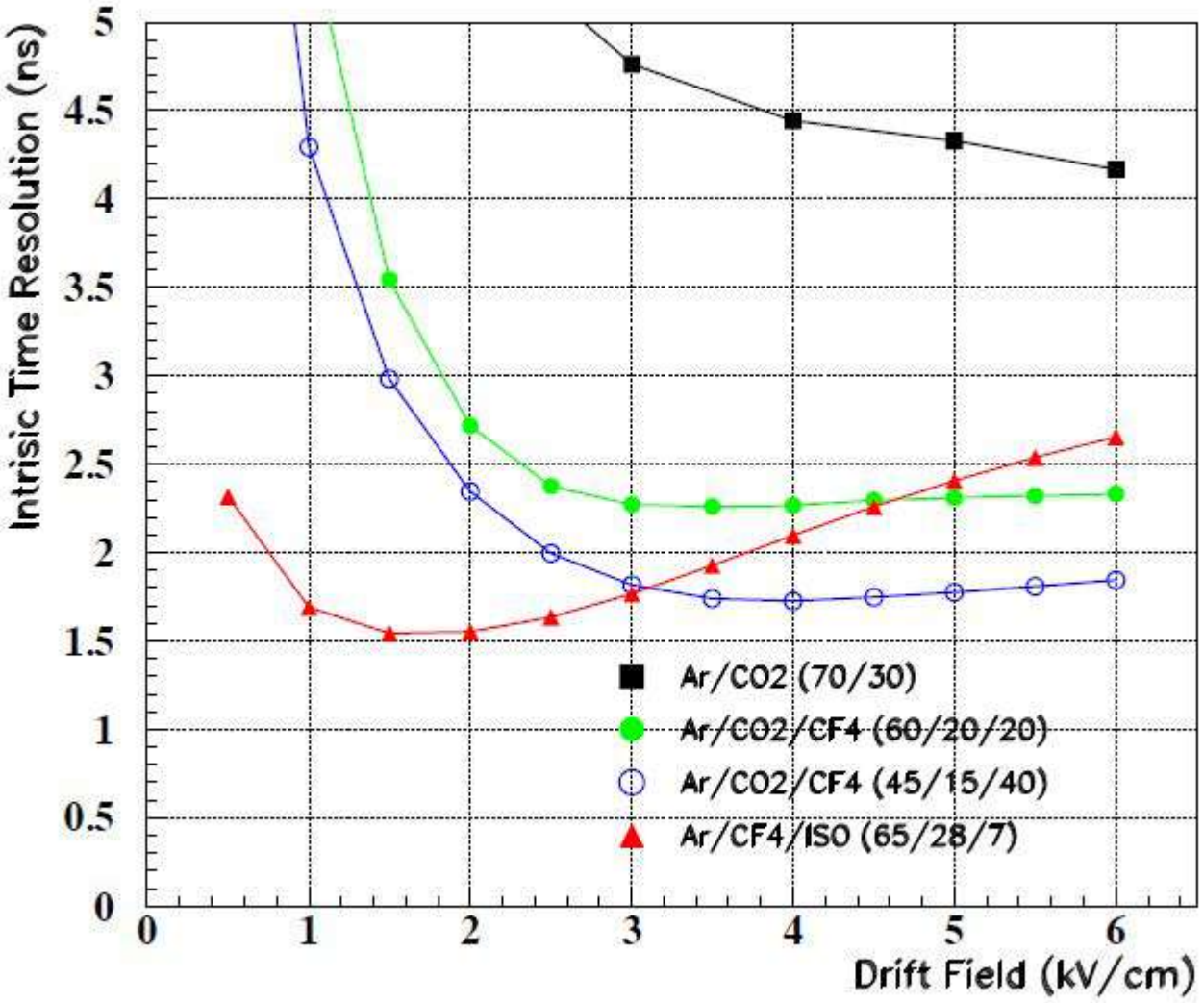

Intrinsic time resolution represents a **lower limit**.

In fact, taking into account
the limited collection efficiency of the first GEM,
the statistical fluctuation of the gas gain
and the finite threshold of the electronics,
it could happen that the signal
induced by the first cluster cannot be discriminated

In this case the successive pile-up of clusters is needed
to have a signal above the electronic threshold

This effect is the main limitation of the detector time resolution

In order to avoid or to reduce this effect, it is necessary to increase
the single electron detection capability.

The use of a fast gas mixture, characterized by a **high drift velocity**
at a relative low value of drift field, which ensures a large collection
efficiency in the first multiplication stage, gives a high detection
efficiency of the first cluster

Signal formation

In triple-GEM detector
the signal is completely induced by the electron motion in the induction gap

As the first electron emerges from the last GEM,
it starts to induce a current on the pads which stops when it is collected

$$i = -\frac{q}{t} = -\frac{qv_d}{x}$$

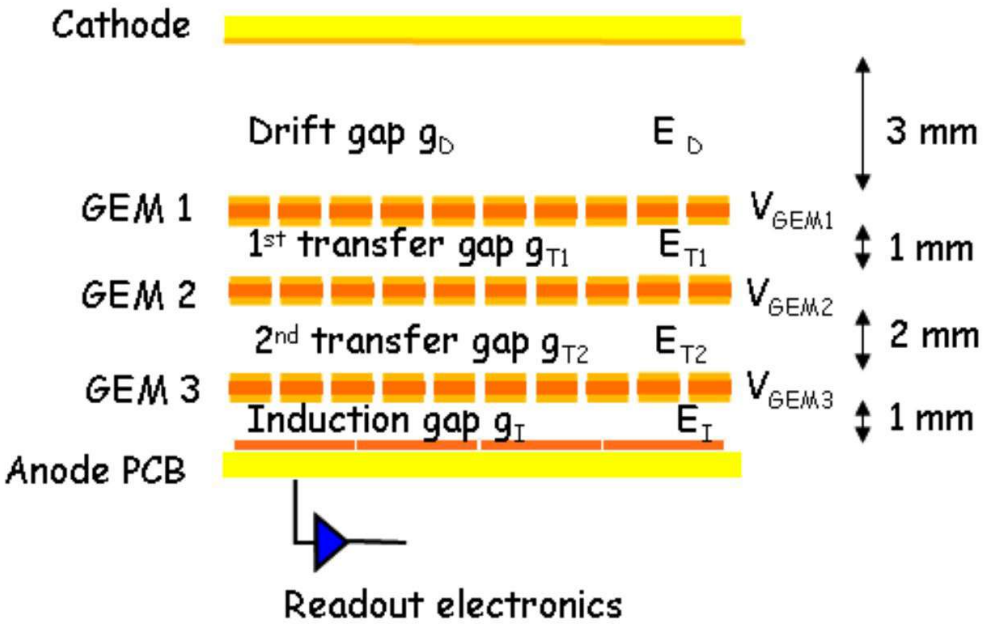

Higher induced signals have been achieved
by reducing the thickness of the induction gap and using a fast gas mixture
for induction field in the range 4.5÷5.5 kV/cm

The R&D activity on triple-GEM detector

Measurements performed in the R&D activity on GEM detectors operated with **CF_4 and isobutane based gas mixture**

The use of such new gas mixtures have also required for the study of the detector capability to tolerate 10 years of LHCb running without damages or performance losses.

Prototype have been realized with three GEM foils **10×10 cm^2 active area** previously stretched and glued on FR4 frames.

The **anode readout has segmented in 6×16 mm^2 pads**

The cathode has made up of a kapton foil, with copper on one side, glued on a similar frame. All frames have then fixed to the FR4 box with nylon screws.

The pads have been connected to a fast preamplifier based on VTX-chip
with a sensitivity of 10 mV/fC, peaking time of 5 ns
and electronic noise charge of about 1300e^- r.m.s at zero input capacitance

The 10×10 cm^2 triple-GEM prototype

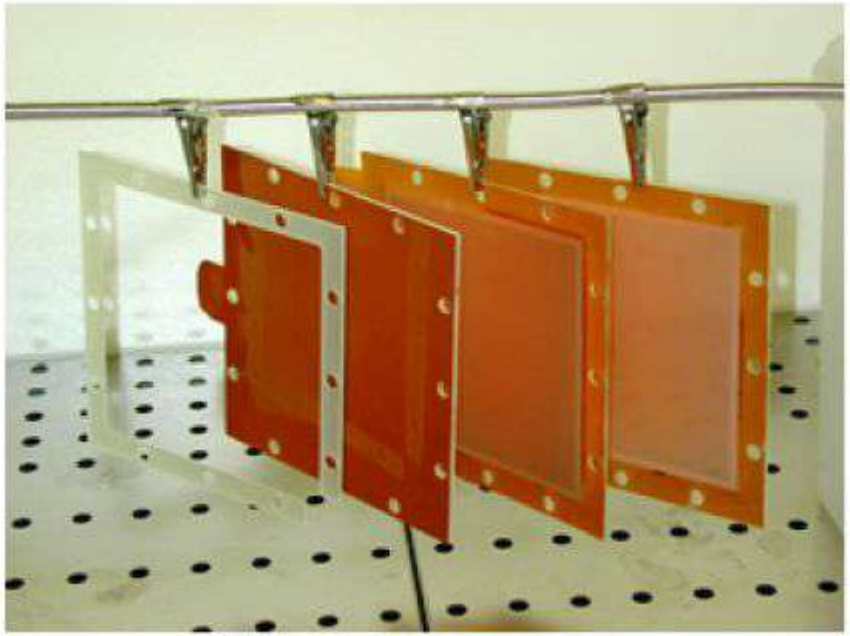

The three GEMs
glued on the FR4 frames
of different thickness

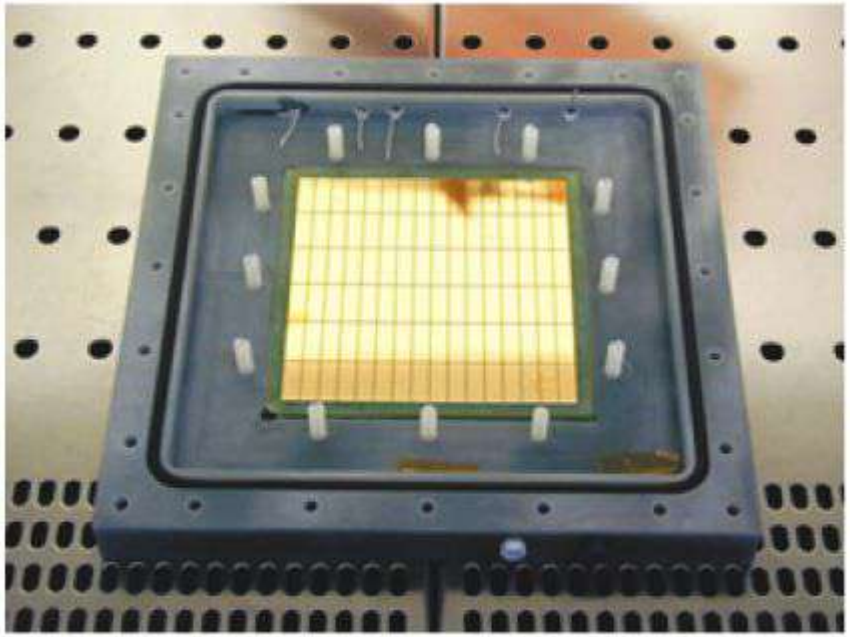

Readout pads
mounted on the FR4 box

The 10×10 cm^2 triple-GEM prototype

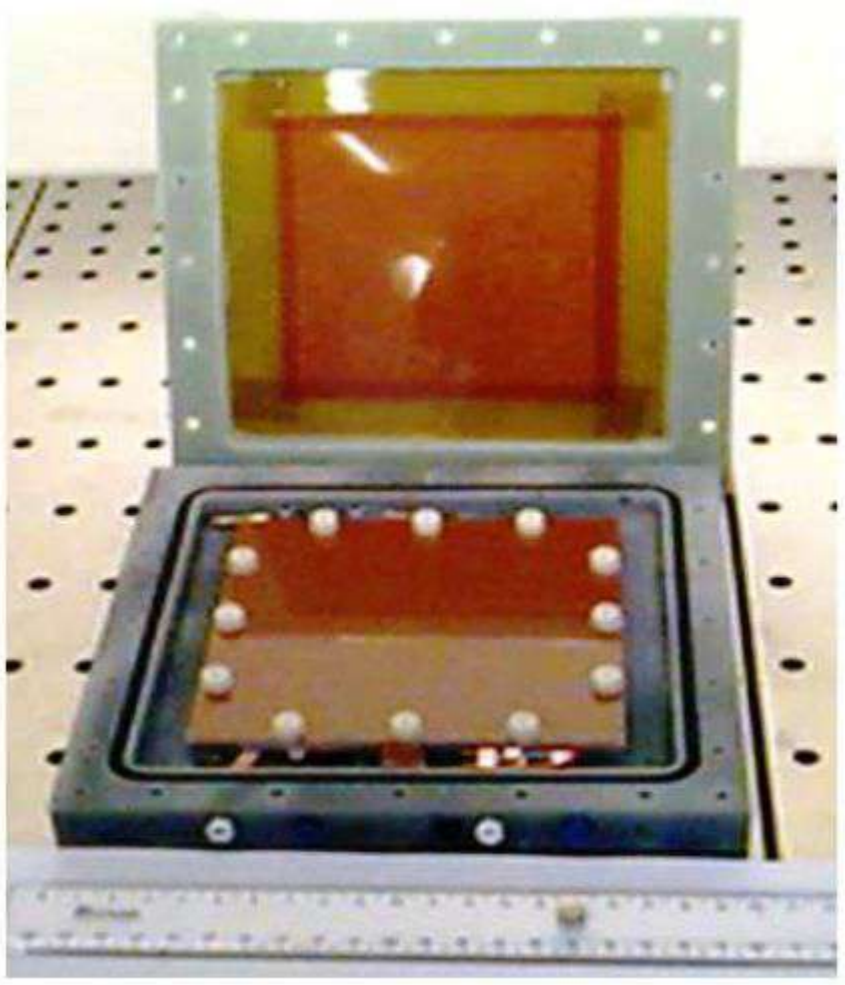

The three GEMs stacked in the FR4 box

Gain measurement

The **effective gain** of a triple-GEM detector

$$G_{eff} \propto e^{<\alpha>V_{GEM}^{tot}}$$

The **gas gain measurement**
has been performed by irradiating a triple-GEM prototype
with a high intensity **6 keV X-ray tube**

The gas gain measurement has been performed by irradiating a triple-GEM prototype with a high intensity 6 keV X-ray tube.
The current induced on the pad I_{PAD}, for a given X-ray flux Φ_{RX} and irradiating area S, is proportional to the detector gain G, through the relation:

$$I_{PAD} = e \cdot N_\gamma \cdot S \cdot \Phi_{RX} \cdot G$$

where e is the electron charge and N_γ is the gas ionization produced by the X-ray, that depends weakly on the gas mixture (≈ 200 electron-ion pair).

Effective particle rate as a function of total GEM voltage for various gas mixtures. The different height of the plateau is due to the different cross sections of the photon conversion in the gas mixture

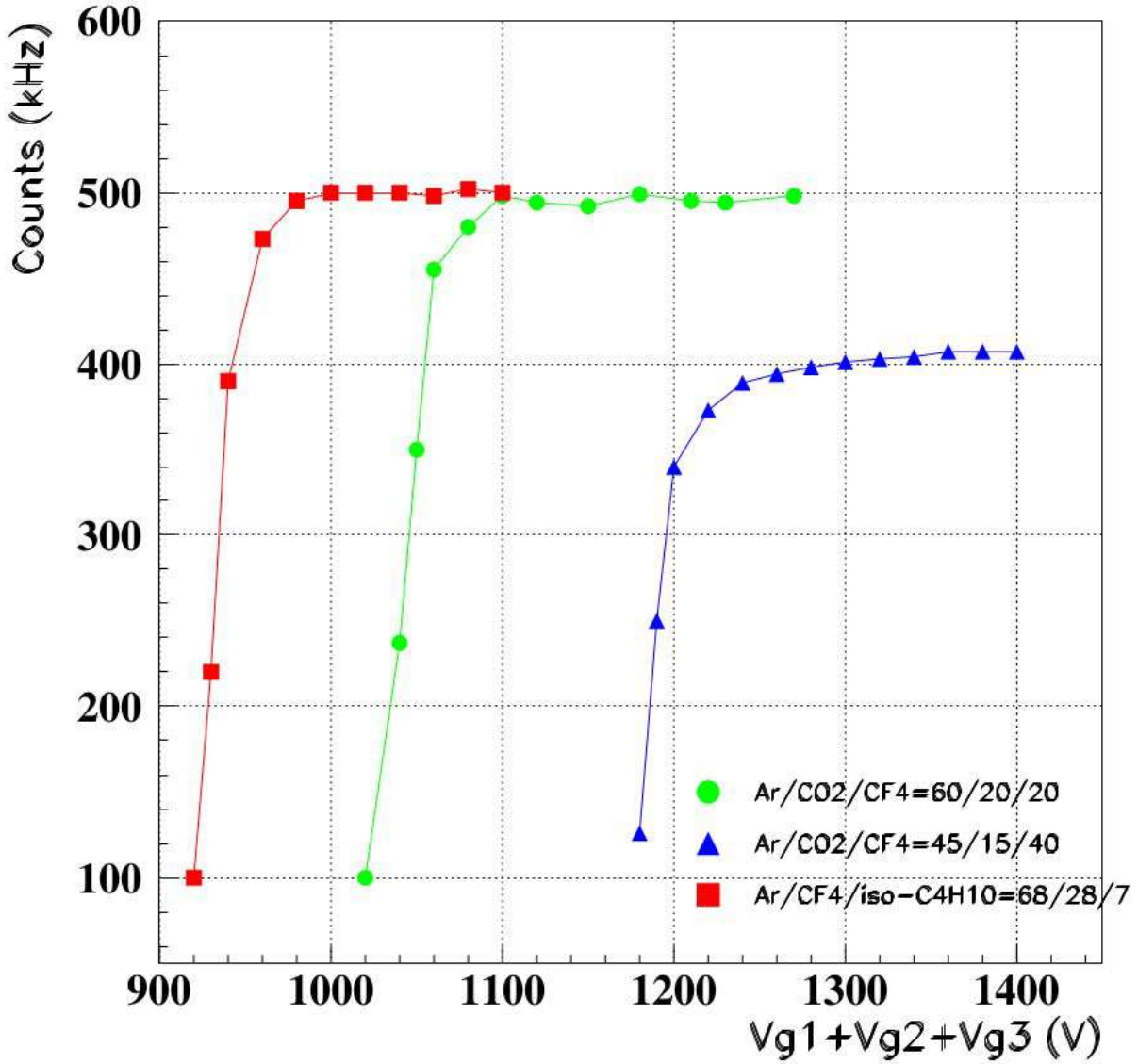

Effective gain of a triple-GEM detector
as a function of total GEM voltage for various gas mixtures

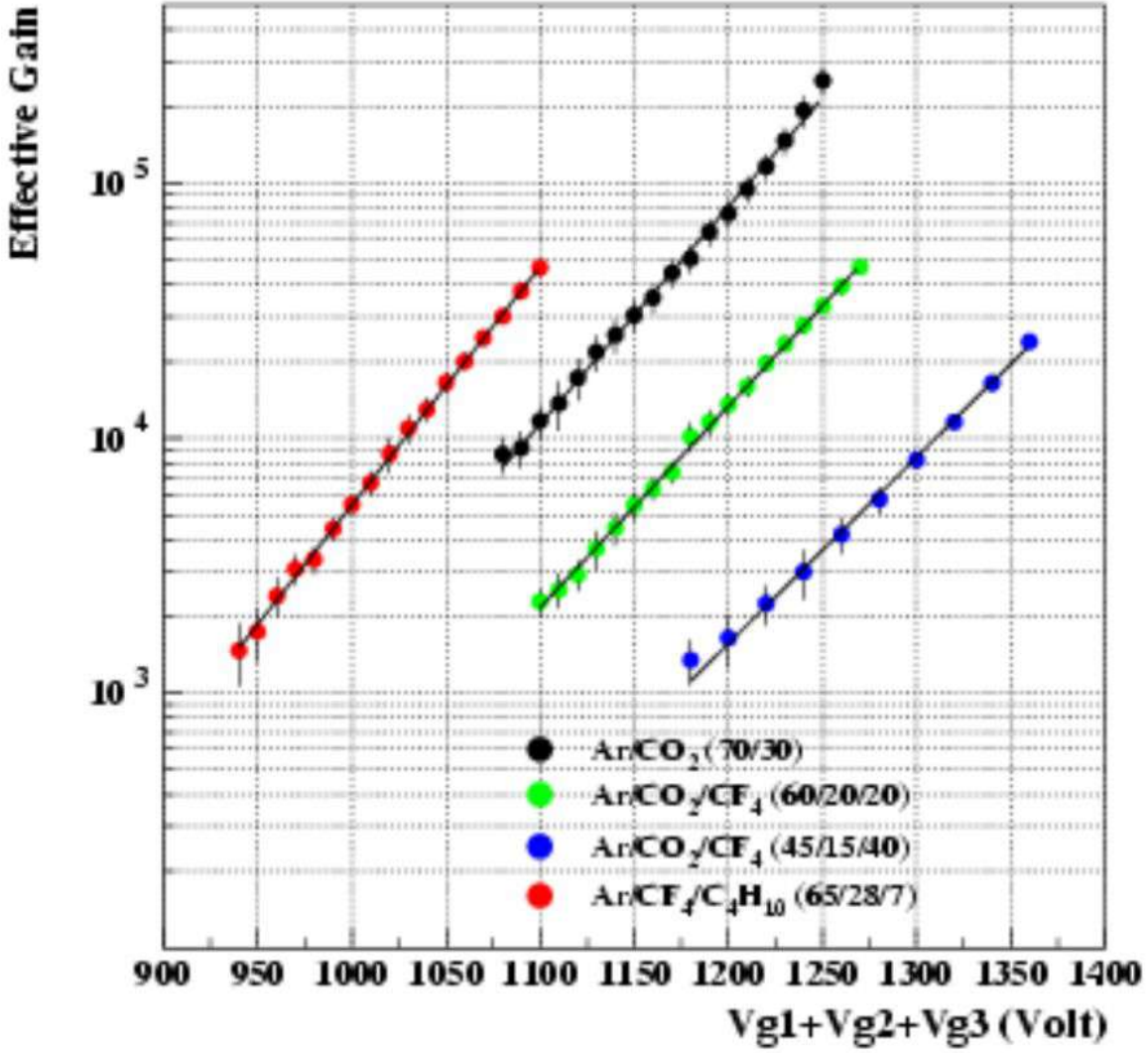

$$G_{eff} \propto e^{<\alpha>V_{GEM}^{tot}}$$

Gas mixture	$< \alpha >$ (V^{-1})
Ar/C0$_2$ (70/30)	19.6×10^{-3}
Ar/C0$_2$/CF$_4$ (60/20/20)	18.2×10^{-3}
Ar/C0$_2$/CF$_4$ (45/15/40)	16.9×10^{-3}
Ar/CF$_4$/iso-C$_4$H$_{10}$ (65/28/7)	21.5×10^{-3}

Rate capability

The rate capability of a detector depends on the time required by the ions to move from the avalanche region to the ion collection electrode.
In a GEM structure the ions produced inside the hole are mainly collected on the upper electrode of the GEM itself in a time of the order of few μs

The detector rate capability has been measured with the **Ar/CO_2/CF_4 (60/20/20)** gas mixture at the **gas gain of 2×10^4**

Gain stability was found up to a particle rate of **60 MHz/cm^2**, showing a very high rate capability and well above the LHCb requirement (500 kHz/cm^2).

This measurement was limited by the maximum flux of the X-ray tube

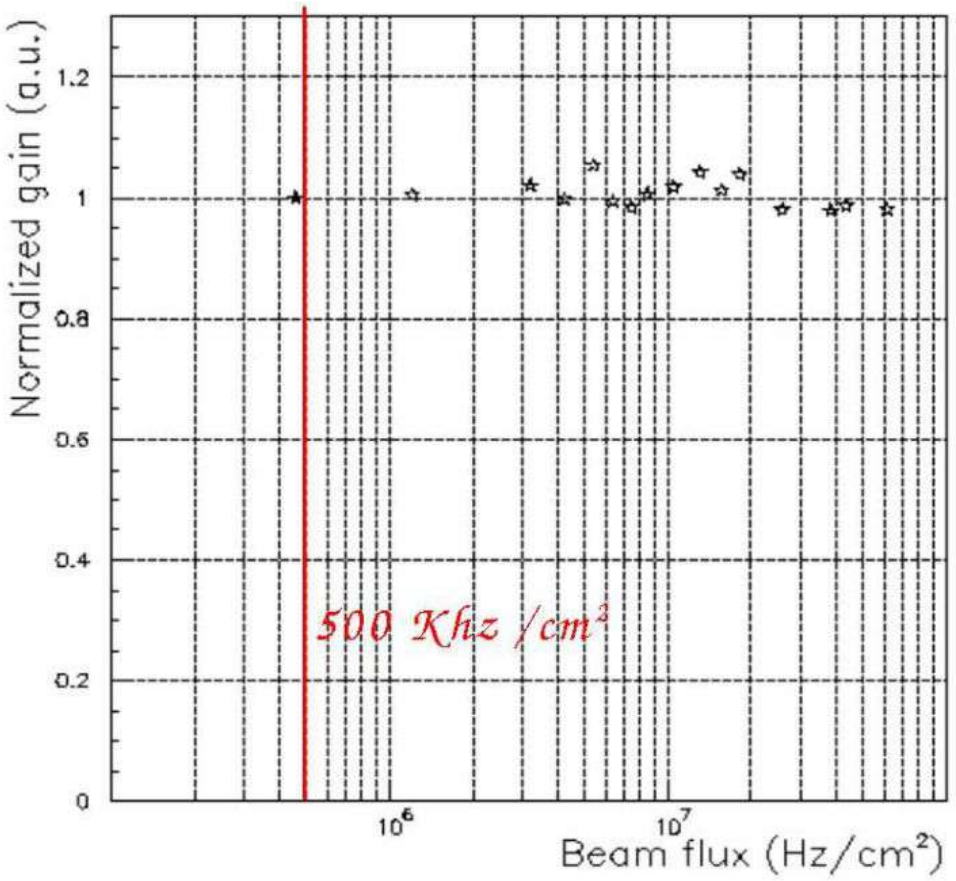

Time and efficiency performances

Several tests have been performed at the T11 beam facility of PS-CERN with π beam of 3÷4 GeV/c.
These tests gave possibility to measure the time performance and the efficiency in 20 ns time window

The best **time distribution**

for single detector

The gas gain was:

1×10^5 for the Ar/CO_2 (70/30);

3×10^4 for the $Ar/CO_2/CF_4$ (60/20/20);

1×10^4 for the $Ar/CO_2/CF_4$ (45/15/40);

2×10^4 for the $Ar/CF_4/iso\text{-}C_4H_{10}$ (65/28/7)

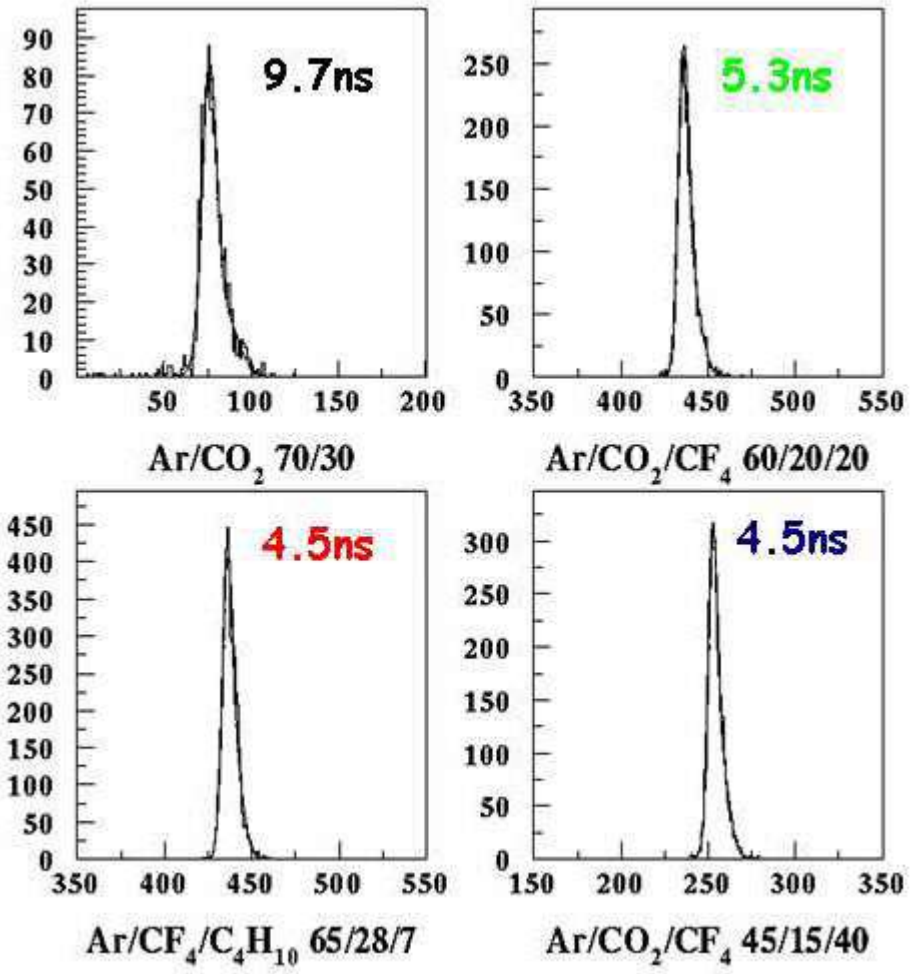

The **electric field configuration**
used during the tests of the gas mixtures

Gas mixture	E_D (kV/cm)	E_{T1} (kV/cm)	E_{T2} (kV/cm)	E_I (kV/cm)
Ar/CO_2 (70/30)	3.0	3.0	3.0	5.0
$Ar/CO_2/CF_4$ (60/20/20)	3.0	3.5	3.5	5.0
$Ar/CO_2/CF_4$ (45/15/40)	3.5	3.5	3.5	5.0
$Ar/CF_4/iso\text{-}C_4H_{10}$ (65/28/7)	2.0	3.0	3.0	5.0

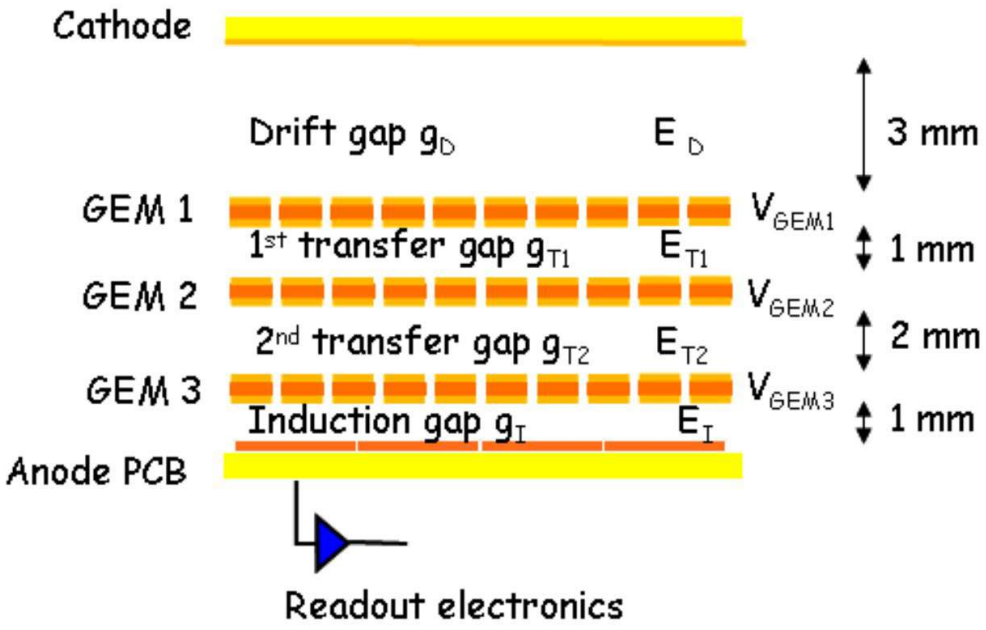

Time resolution measurement for a single detector

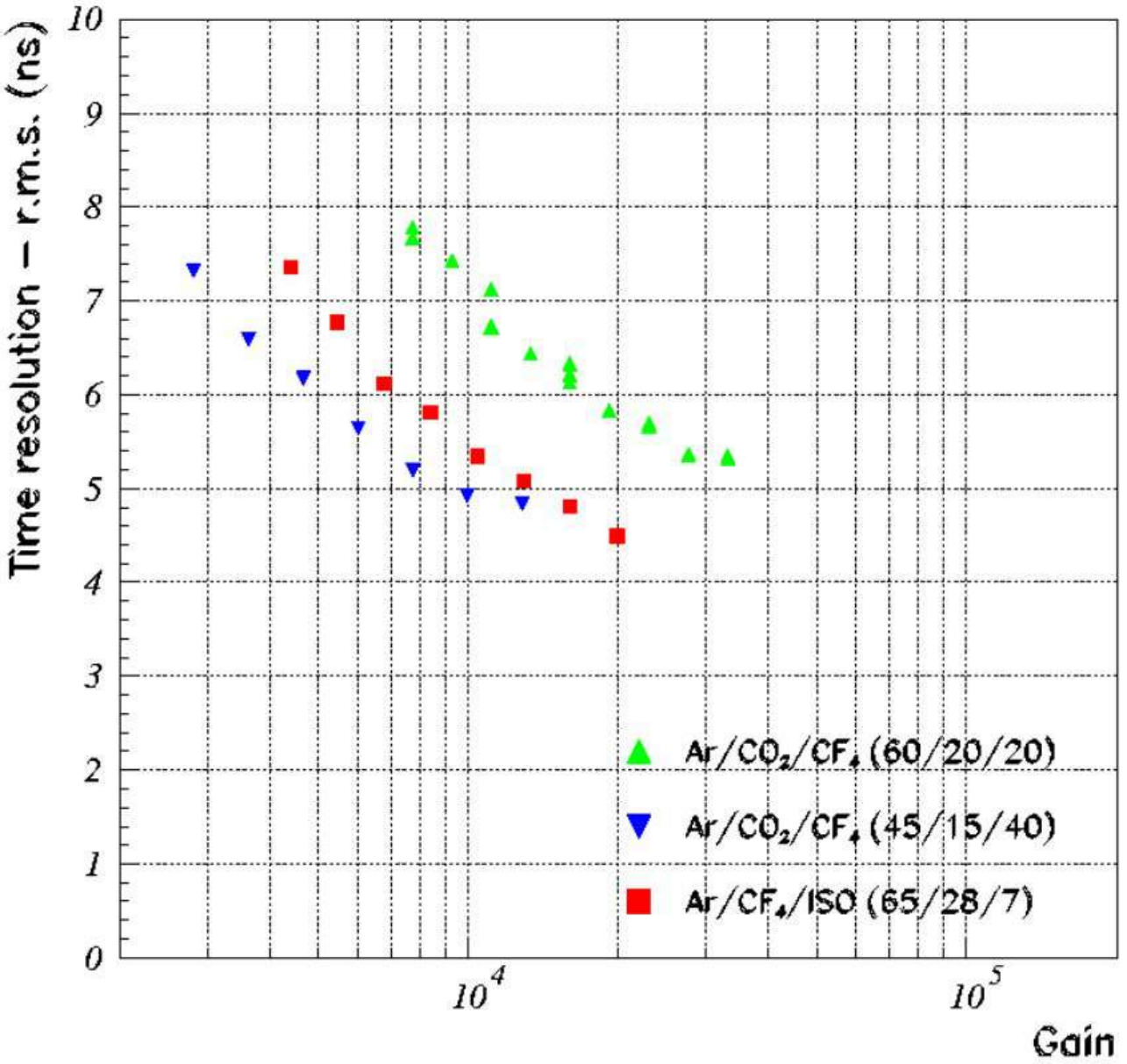

Time resolution measurement for two detectors logically OR-ed, as foreseen in the LHCb experiment.

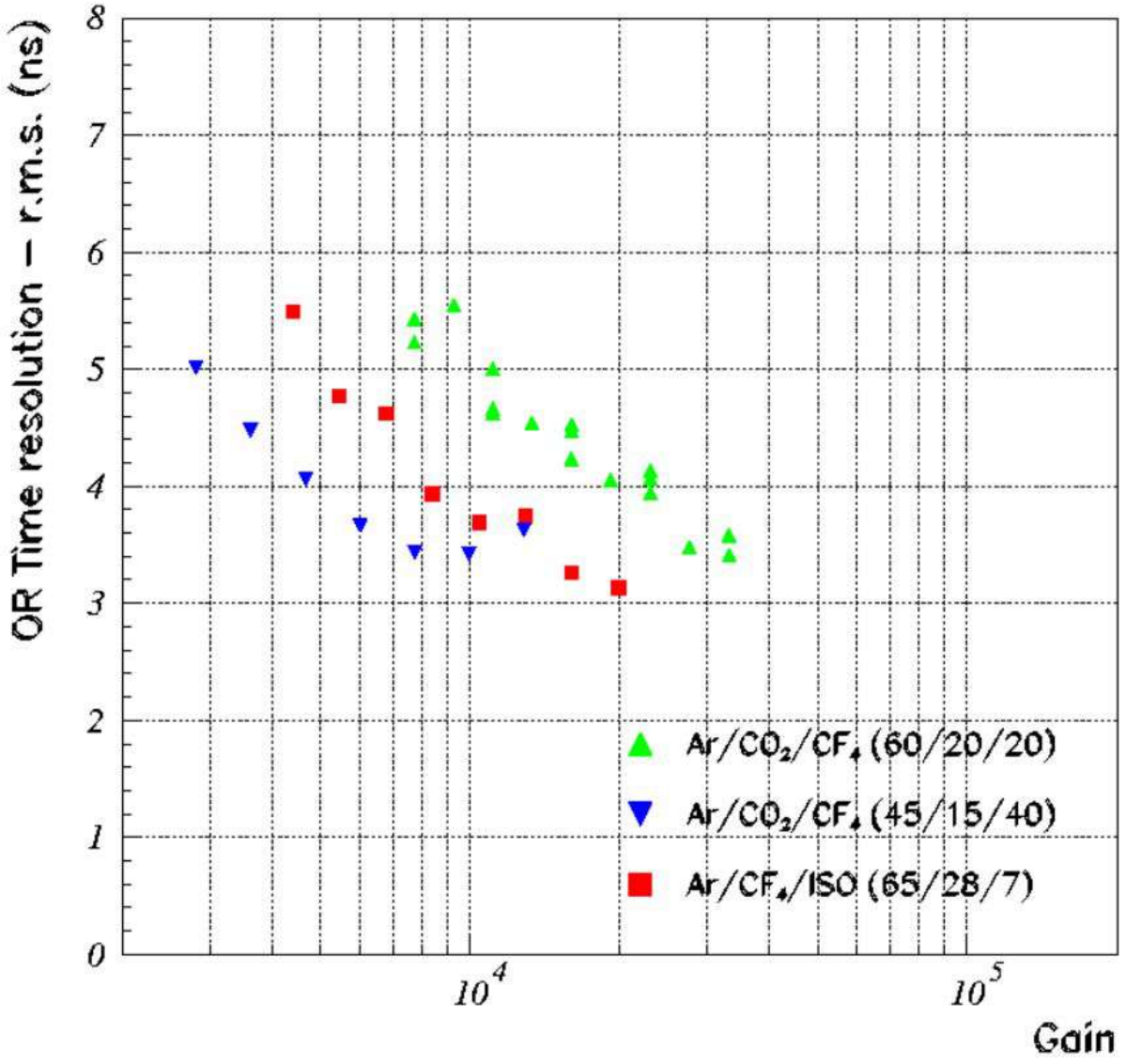

The efficiency in 20 ns time window as a function of the effective gain **for a single detector**

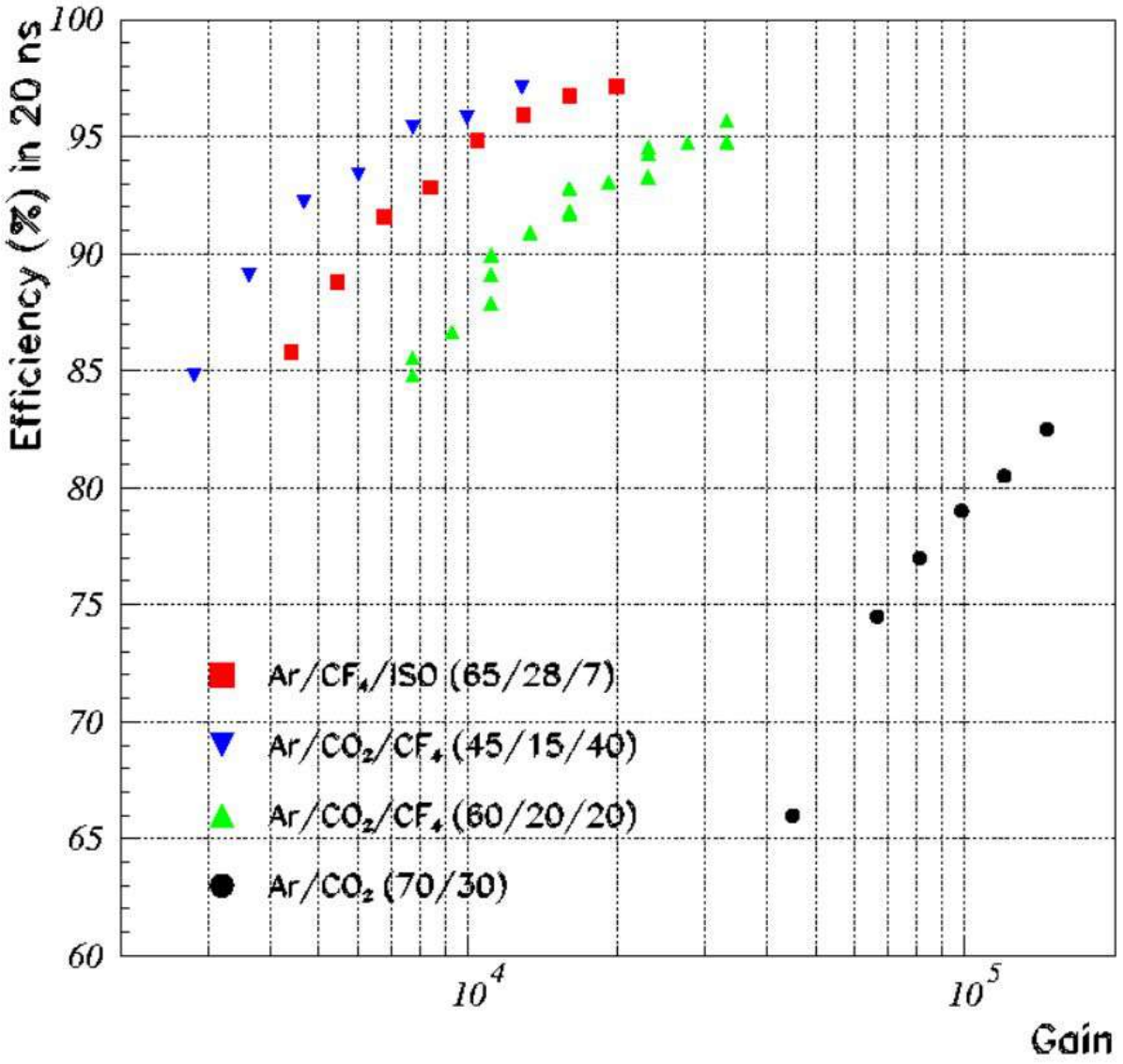

The efficiency in 20 ns time window as a function of the effective gain **for two detectors logically OR-ed** as foreseen by the experiment LHCb

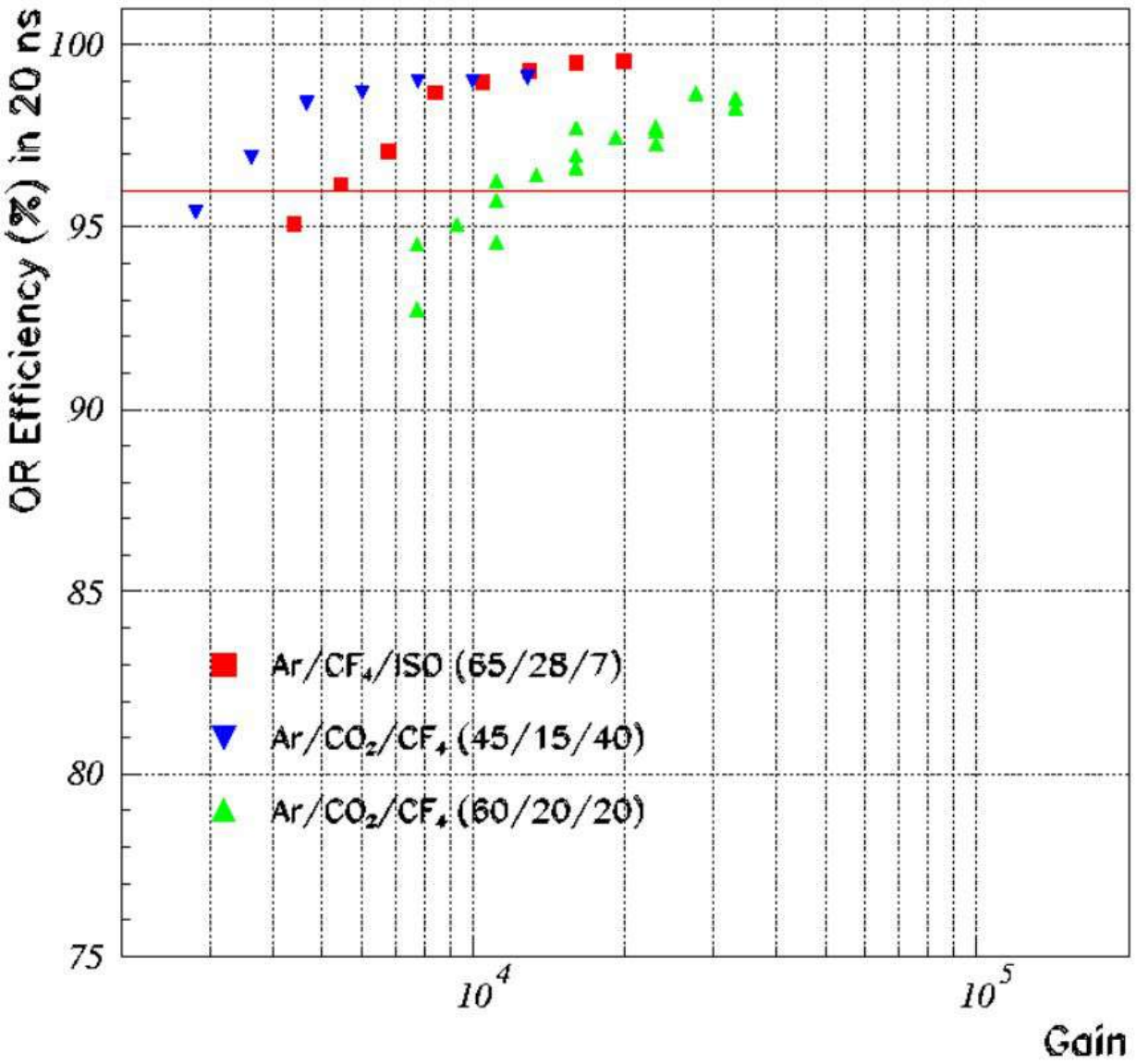

Discharge probability per incident particle

as a function of the effective gain for a detector with 3/1/2/1 gap geometry

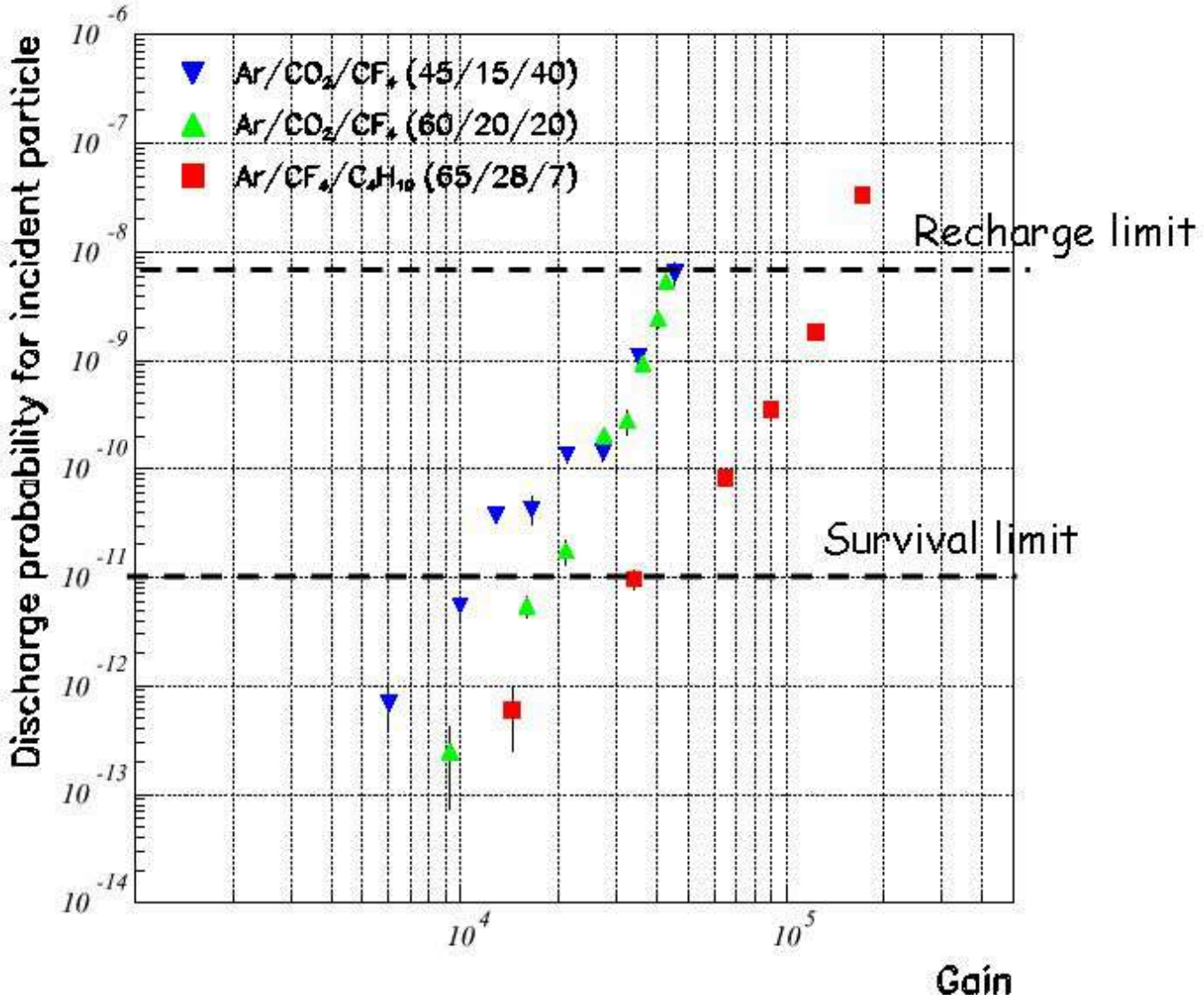

Ageing tests

The chemistry of the ageing process has not been yet deeply studied thus a rigorous explanation of why certain chambers age and others do not cannot be yet discussed with certainty.

The approach to the ageing problem is still in most cases purely experimental.

It should be stressed that ageing test should be performed as close as possible to the real conditions.

Consequently, the irradiated area of the detector should be as large as possible while the detector should be operated with a gas flow and radiation flux which are comparable to those foreseen in the experiment.

Of course for time constraints such tests must be accelerated, then a radiation flux several times higher than the foreseen one have to be used, often affecting the reliability of the results.

Ageing tests

The charge integrated
in 10 years of LHCb running (Δt_{LHCb}) has been estimated as follows:

$$Q_{LHCb}^{integrated} = 2 \cdot \Phi_{LHCb} \cdot \Delta t_{LHCb} \cdot e \cdot N \cdot G$$

where the factor 2 takes into account that the integrate charge is by means the sum of the currents induced on the pads readout and the bottom electrode of the third GEM (G3 D), Φ_{LHCb} is the average charged particle flux expected flux in M1R1 (460 kHz/cm^2) , e is the electric charge (1.6×10^{-19} C), N is the specific ionization that is estimated to be $\sim$ 40 electron-ion pair for all the gas mixtures and G is the gas gain used in the test.
Tab. 3.4 summarizes the values of the gas gain, the integrated charge and the equivalent LHCb years of running for each of the gas mixtures tested.

Gas mixtures	Gas gain	Integrated charge (C/cm^2)	Equivalent LHCb years
Ar/CO_2/CF_4 (60/20/20)	2×10^4	20	$\sim$ 16 years
Ar/CO_2/CF_4 (45/15/40)	6×10^3	4.2	$\sim$ 11 years
Ar/CF_4/iso-C_4H_{10} (65/28/7)	1×10^4	10.2	$\sim$ 15 years

Normalized gain as a function of the integrated charge (PAD + G3 D) for the **$Ar/CO_2/CF_4$ (60/20/20)** gas mixture
The detector gas gain has been set at 2×10^4
The red line indicates the integrated charge corresponding to 10 years of operation at LHCb.

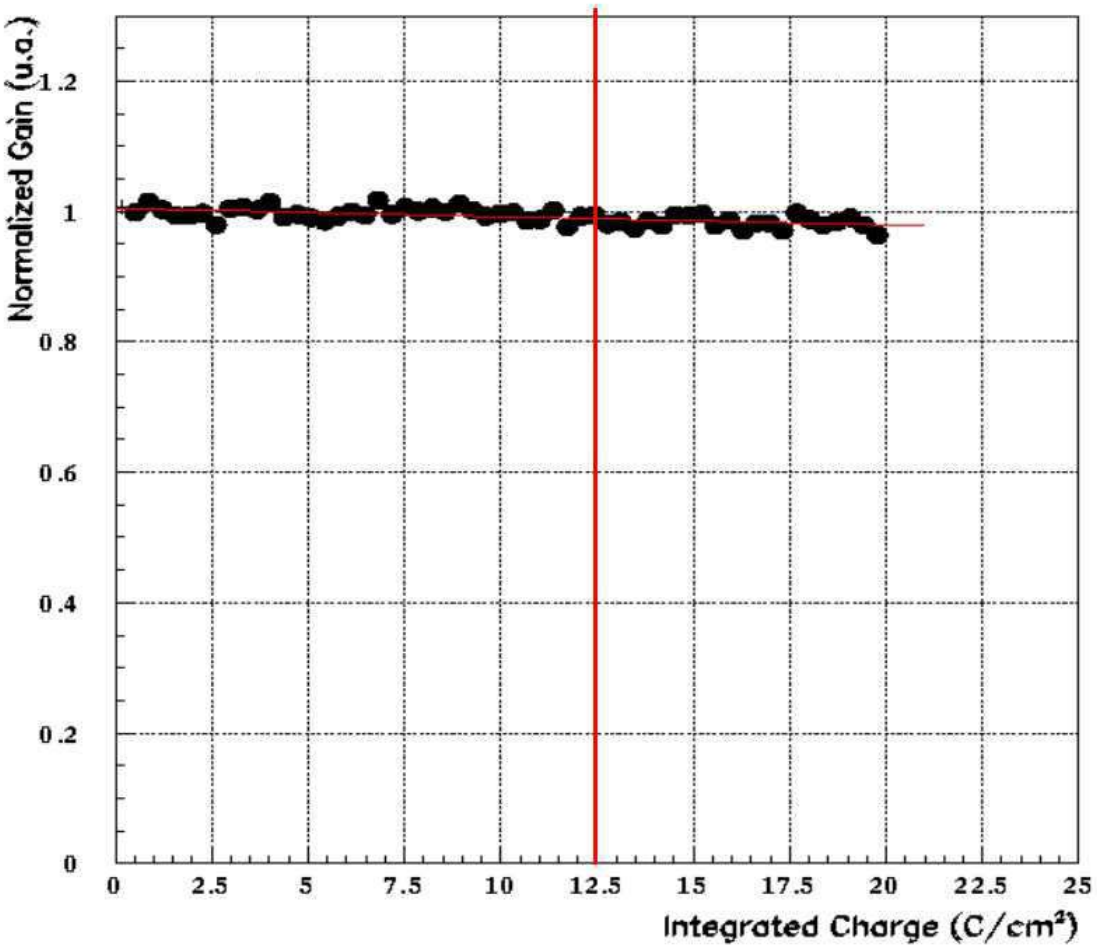

Normalized gain as a function of the integrated charge (PAD + G3 D) for the **$Ar/CO_2/CF_4$ (45/15/40)** gas mixture
The detector gas gain has been set at 6×10^3
The red line indicates the integrated charge corresponding to 10 years of operation at LHCb.

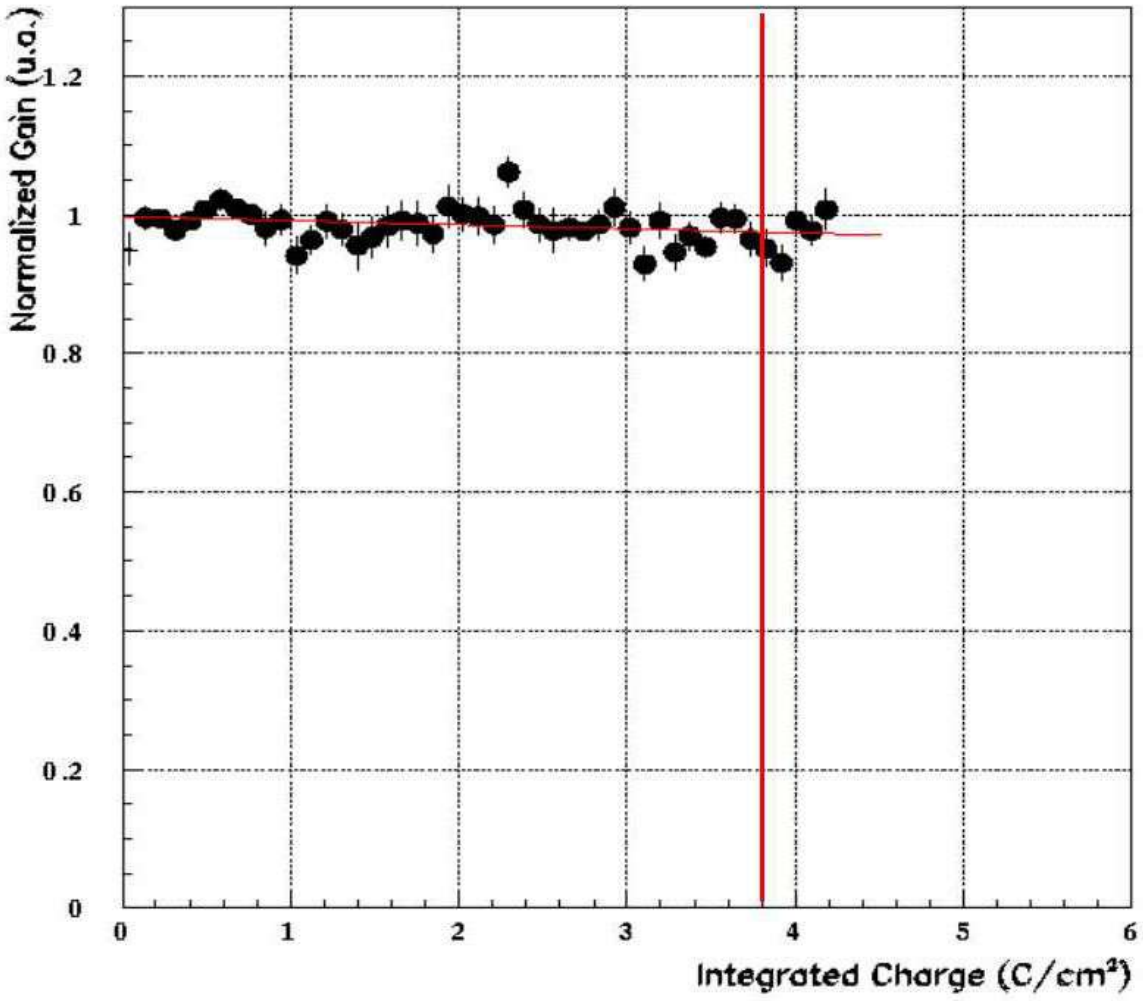

Normalized gain as a function of the integrated charge (PAD + G3 D) for the **Ar/CF_4/iso-C_4H_{10} (65/28/7)** gas mixture
The detector gas gain has been set at 1×10^4
The red line indicates the integrated charge corresponding to 10 years of operation at LHCb.

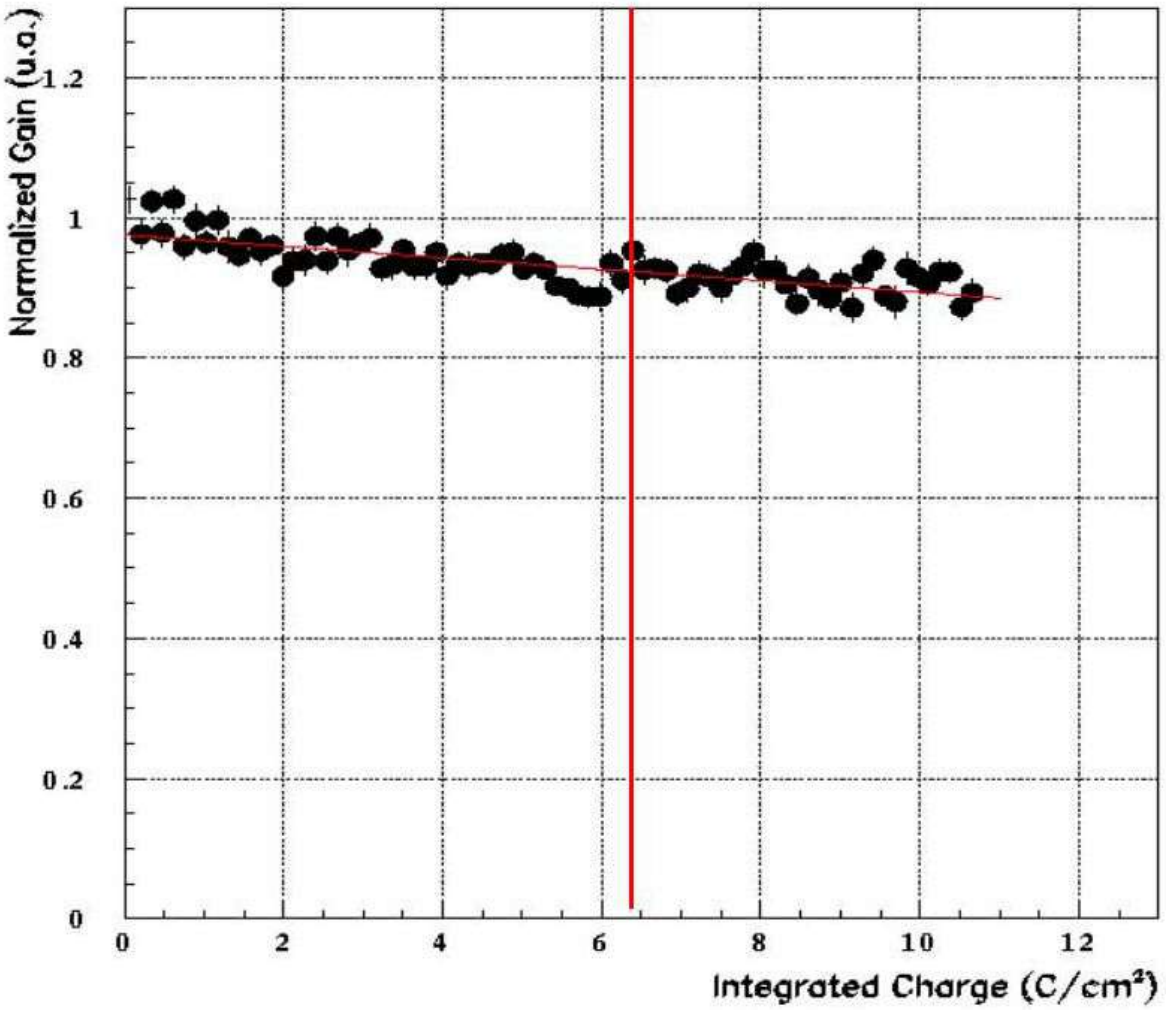

Conclusions of the R&D activity on the triple-GEM detector 10×10 cm^2 of active area

The detector shows very high rate capability above the maximum rate at LHCb.

Optimization to improve the detector efficiency in 20 ns time window

Time resolutions better than 5 ns are achieved with fast and high yield CF_4 and iso-C_4H_{10} based gas mixtures, considerably improving the results obtained in the past with the standard Ar/CO_2 (70/30) gas mixture (~ 10 ns).

With these new gas mixtures, the detector achieves an efficiency in 20 ns time window above the 96% at moderate gas gain, while keeping the discharge probability per incident particle lower than ~ 5×10^{-11} .

Gas Ar/CO_2/CF_4 (45/15/40) as the reference gas mixture for the GEM LHCb experiment

The triple-GEM detector in LHCb

The total area of M1R1 region, about 0.6 m^2, will be covered with 12 stations composed by two triple-GEM detectors logically OR-ed pad by pad.
The active area of each station is 200×240 mm^2.

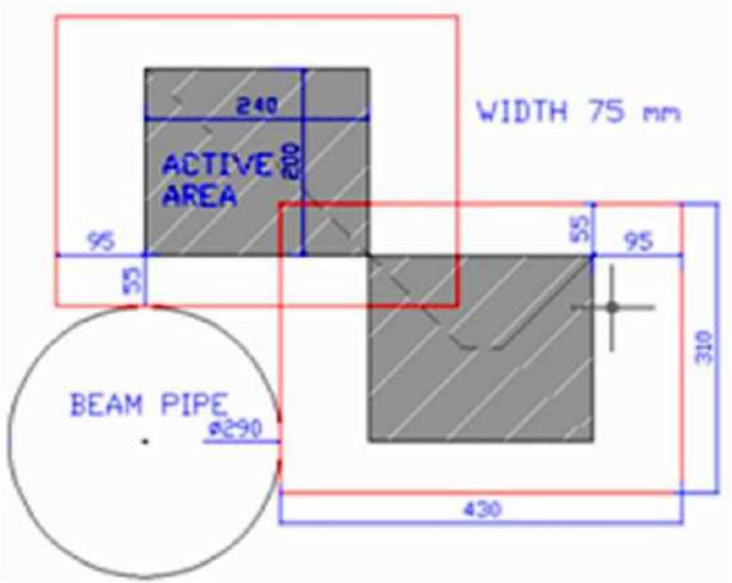

Transverse view, with respect to the LHC beam axis, of the geometrical envelope of 2 out of the 12 stations, together with the chamber active area,
the panels and the electronics dimension

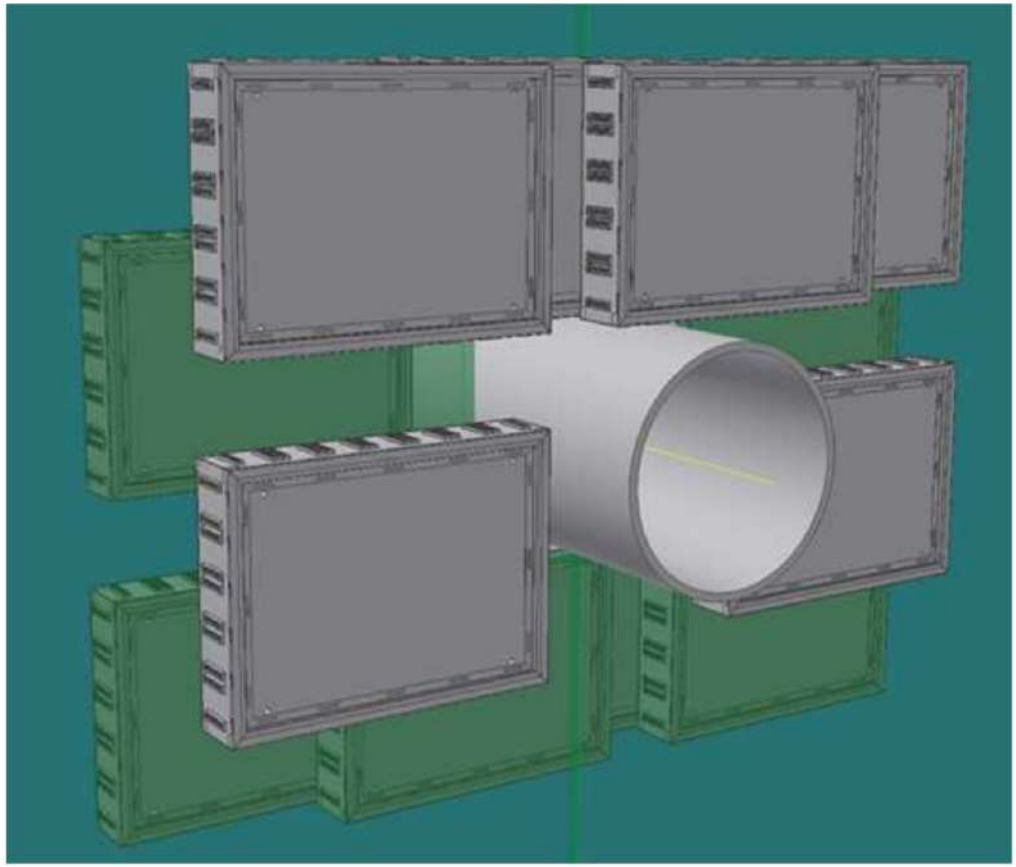

Sketch of the station arrangement in M1R1 region in the x-y plane. The two sets of detector stations, upstream and downstream the wall support structure, are shown with different colors.

Station arrangement
in M1R1 region
in the z plane

The stations must fit
into the 37 cm space
available between the RICH2
and the Preshower

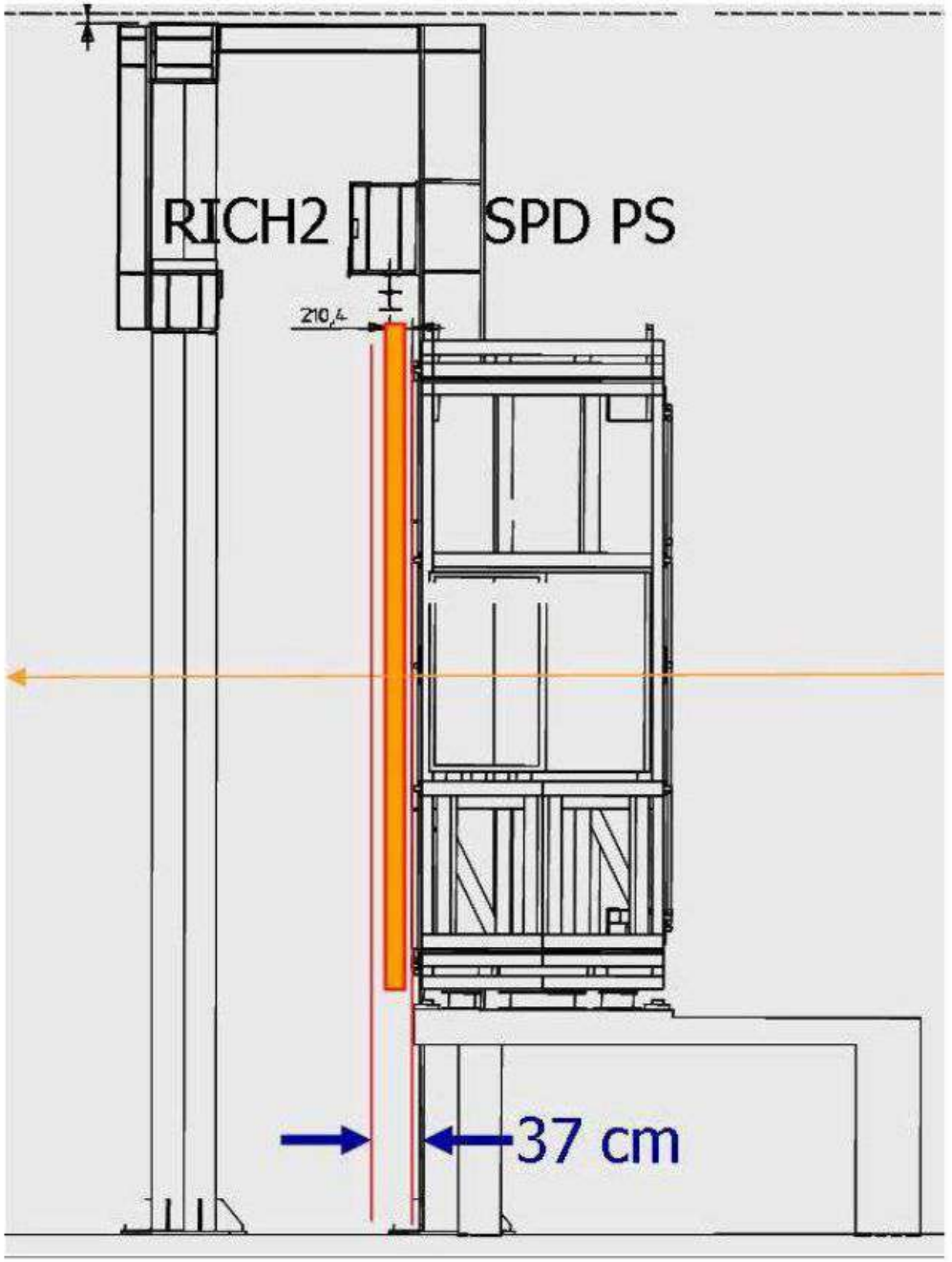

Detector requirements

The detector requirements that a triple-GEM station have to fulfill in M1R1 region are:

- a particle rate capability up to 500 kHz/cm^2;
- each station must have an efficiency higher that 96% within 20 ns time window;
- a pad cluster size, i.e. the number of adjacent detector pads fired when a track crosses the detector, should not be larger than 1.2 for a 10×25 mm^2 pad size;
- the detector must tolerate, without damages or performance losses, an integrated charge of ~ 1.8 C/cm^2 in 10 years of operation at a gas gain of $\sim 6\times10^3$ and an average particle flux of 184 kHz/cm^2 for an average luminosity machine of 2×10^{32} cm^{-2} s^{-1};

Material budget distribution in percentage of X_0 in the overlap of three stations

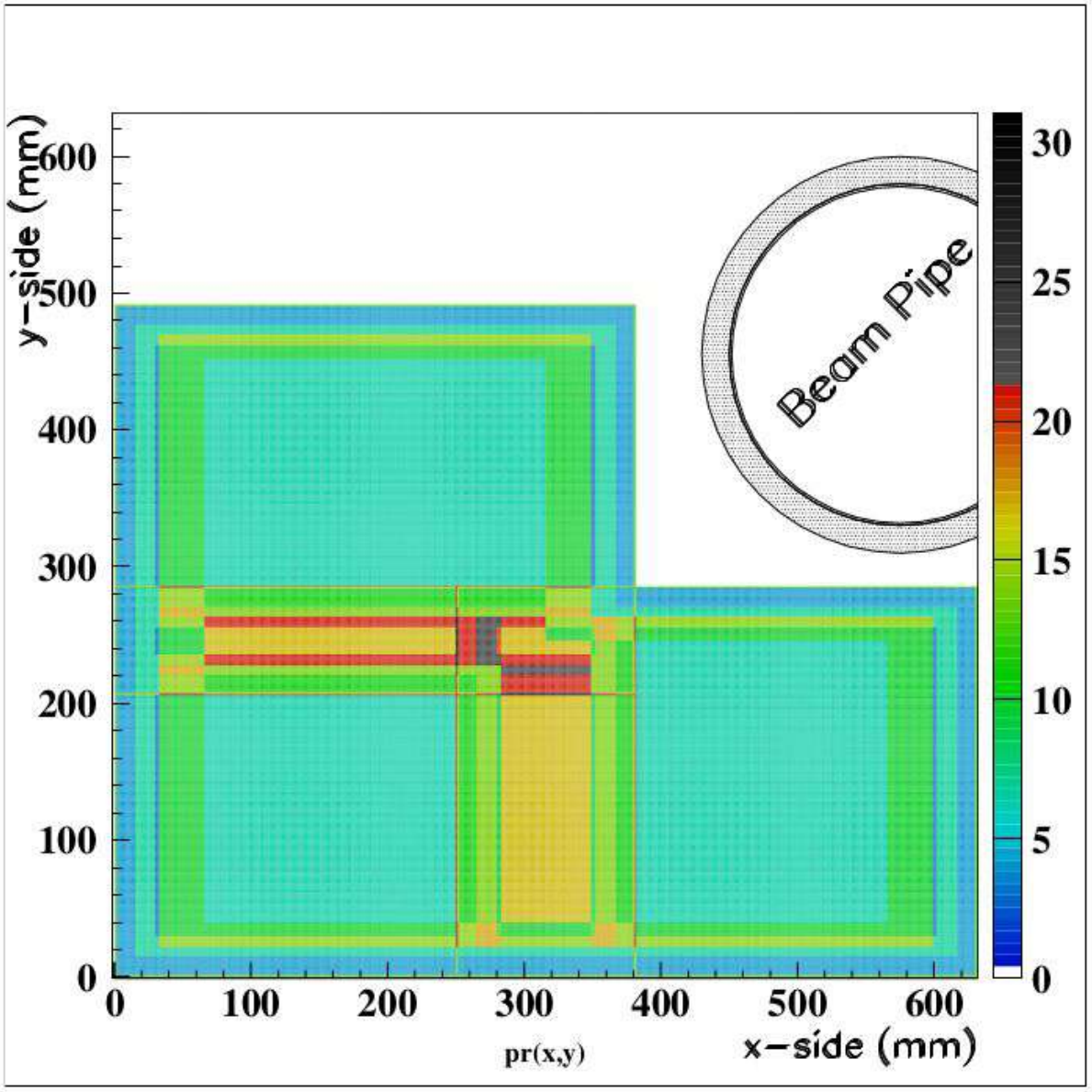

The pad-readout panel

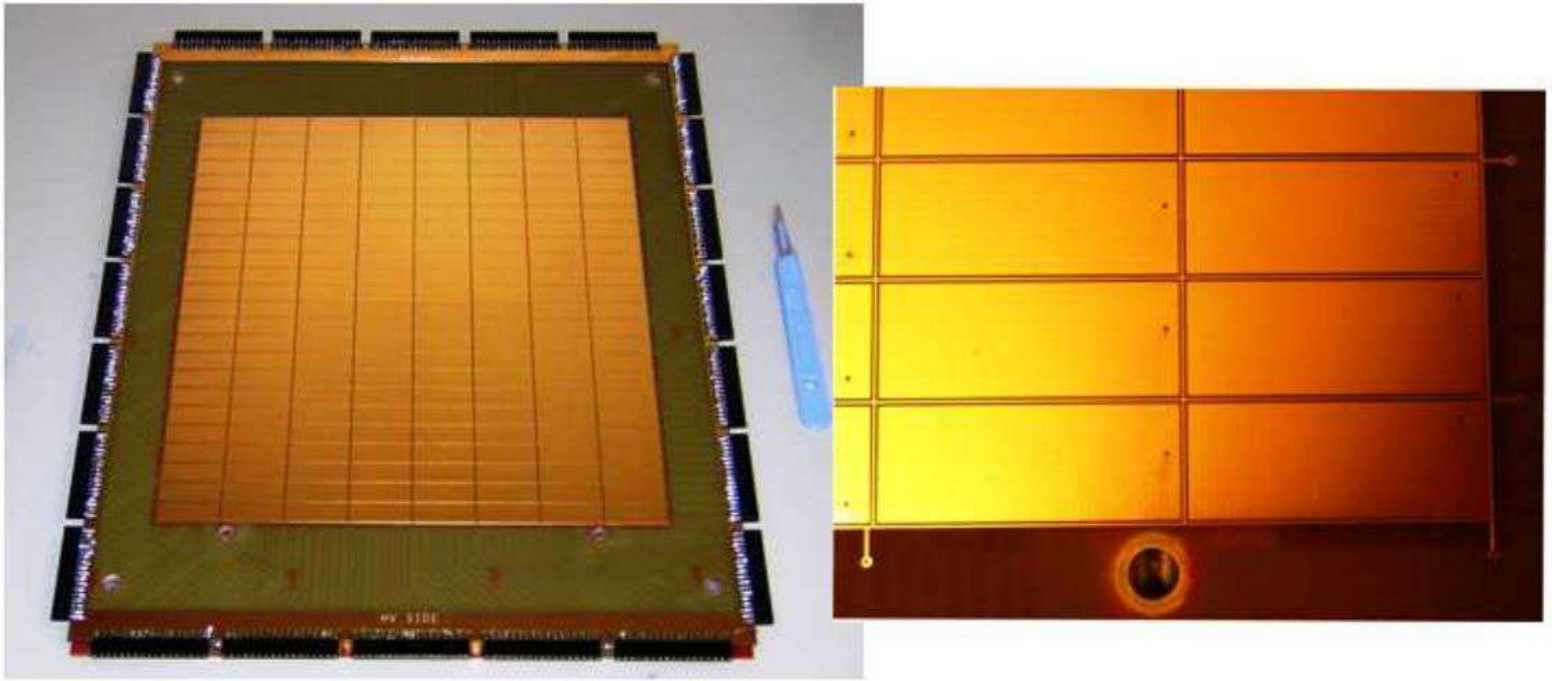

The pad readout: the gold-plated pad matrix of 200×240 mm^2 represents the active area of the chamber.
A close view of the insert gas and the ground grid between the pads is shown in the right picture

Station pad layout as view from the L0 muon trigger

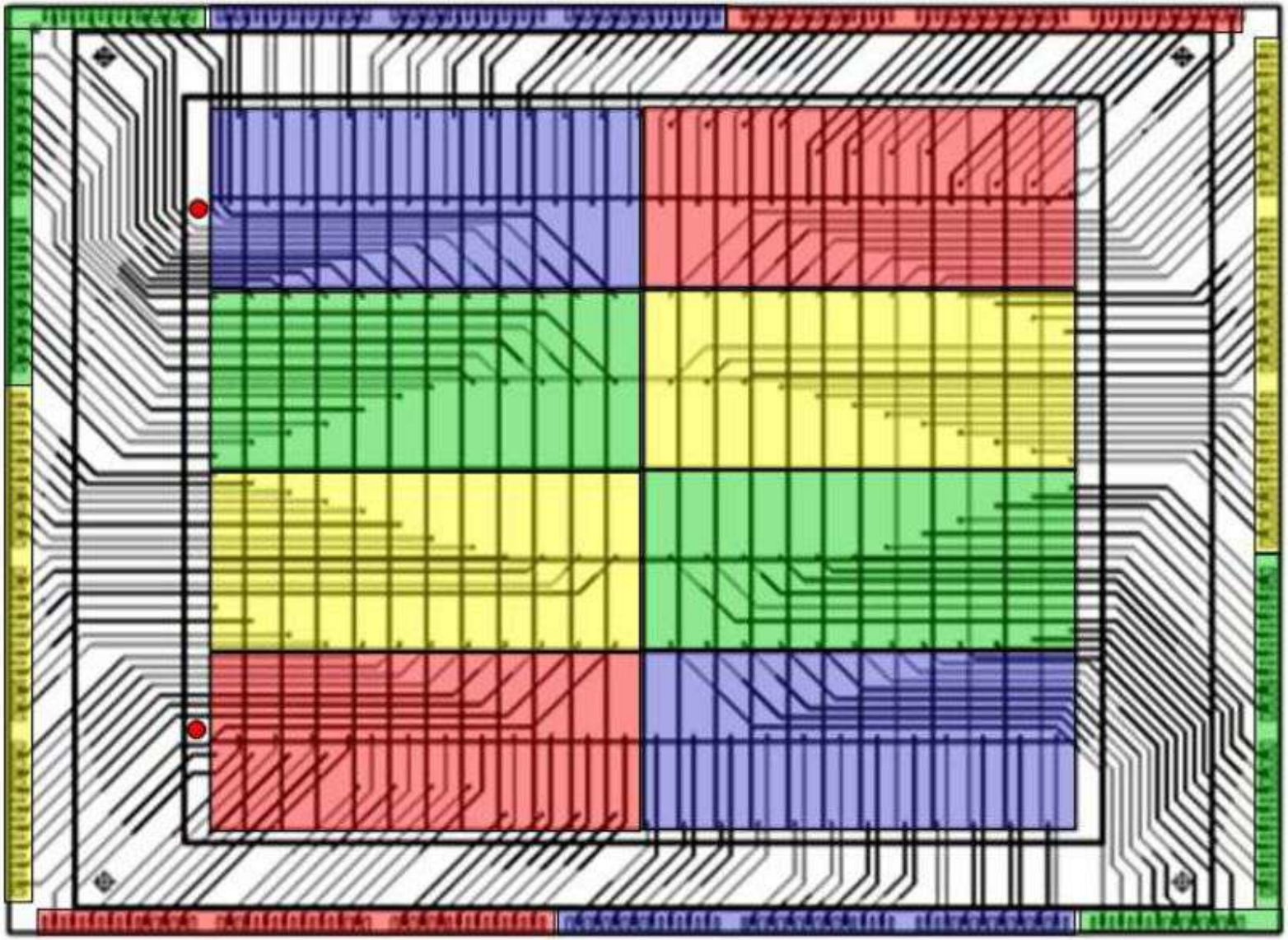

The GEM foil

In order to reduce the energy stored on the GEM and the discharge propagation,
one side of the foil has been divided in six sectors, while the other side is not segmented.
The separation between sectors is 200 μm

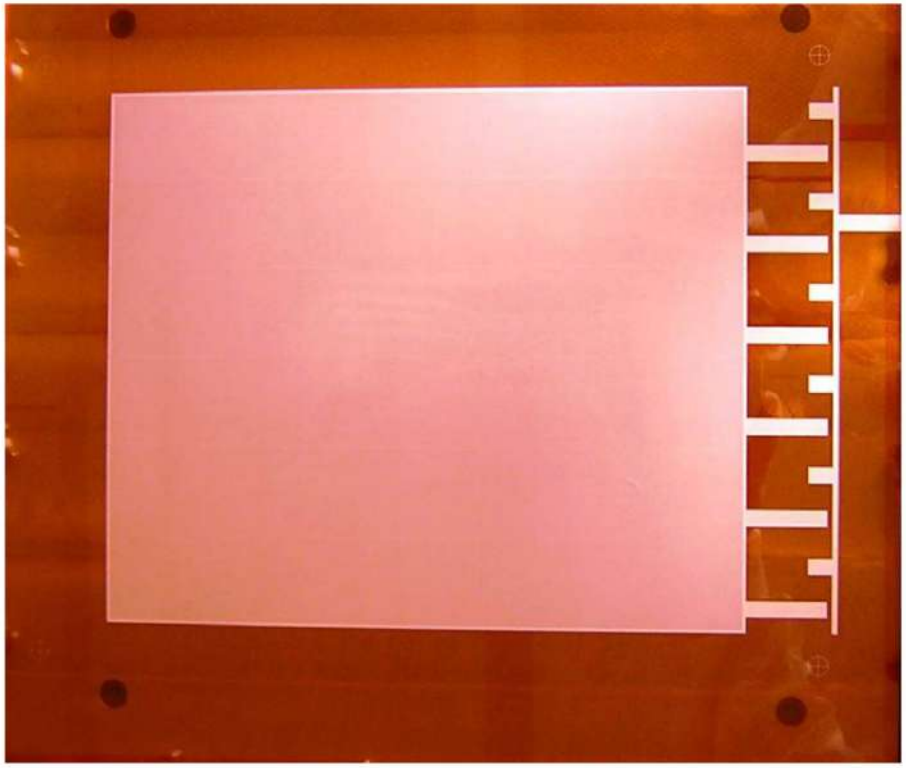

A GEM foil as seen from the segmented side.
The HV connections are visible on the right of the picture

Assembly of triple-GEM detector

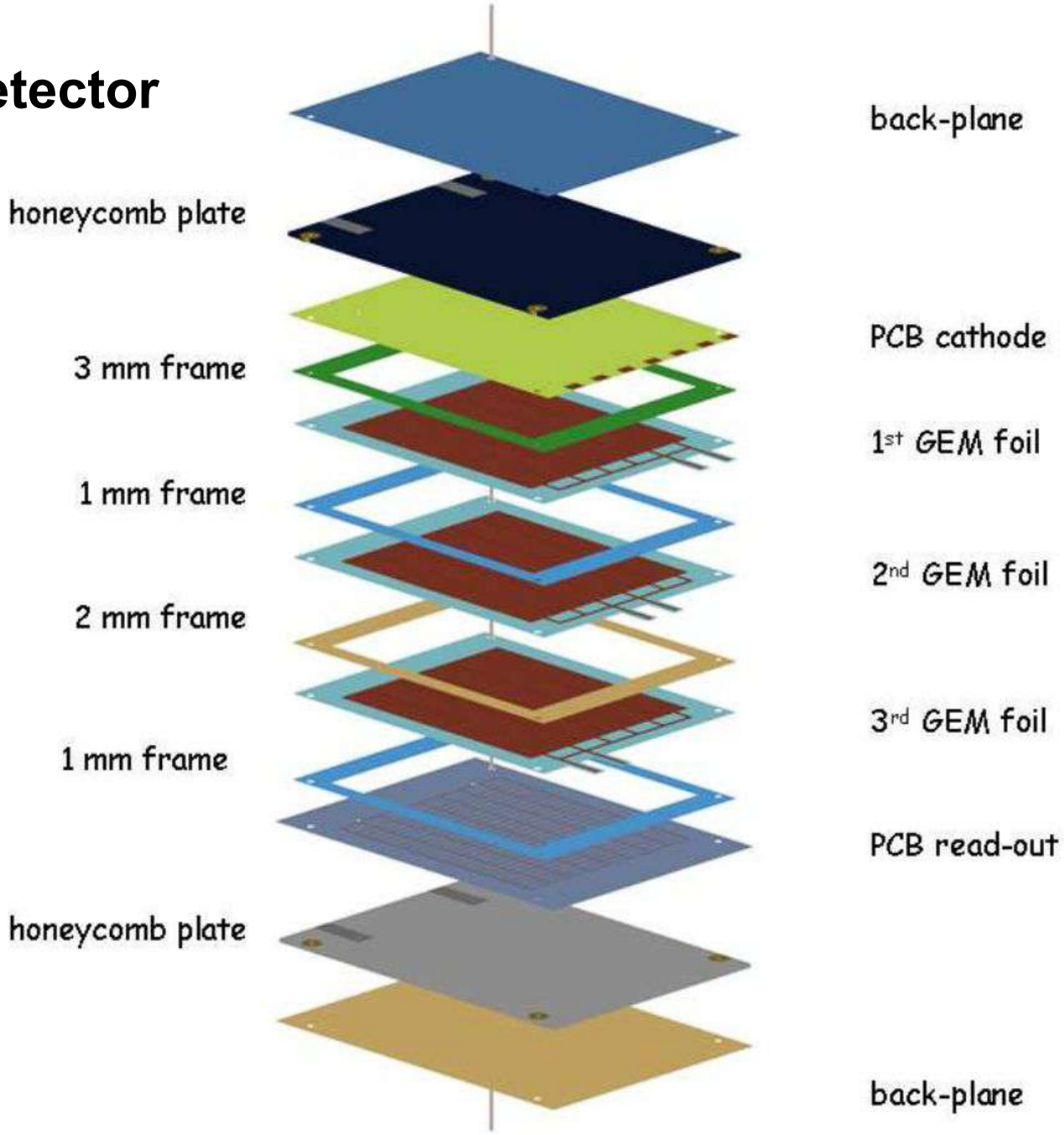

The stretching of the GEM foil

The electrostatic attraction between the electrodes of two consecutive GEM foils could produce a sag of the foil itself, including electrostatic instability such as foil oscillation, and giving rise to possible discharges and local gas gain changes.

To avoid electrostatic instability and to achieve a good uniformity response, we chose to stretch the GEM foil.
The mechanical tension applied to the GEM foil
and its behavior as a function of time have been investigated with various tests.

Electrostatic attraction effect

If electric field is 5 kV/cm
between two consecutive foils,
then pressure due to
electrostatic force is ~1 Pa

$$p = \frac{\epsilon_0 \epsilon E^2}{2}$$

Mechanical tension tests

To estimate the sag produced by 1 Pa on a GEM foil, previously stretched at 20 MPa, a uniformly distributed load of 0.8, 1.6 and 2.4 N is applied.

Using the 3-D machine, the foil bending is measured on a grid of 25 points

Since a load of 1 N distributed over an area of 400×400 mm^2 , equivalent to ~ 6 Pa, gives a sag of ~ 100 μm and since the sag linearly depends on the mechanical pressure, the electro-static pressure of ~ 1 Pa will produce a sag of ~ 15 μm.

It should be stressed that such estimation represents an upper limit for the actual sag of a stretched foil because the two opposite forces, symmetrically applied to each GEM foil, result in a vanishing sag.

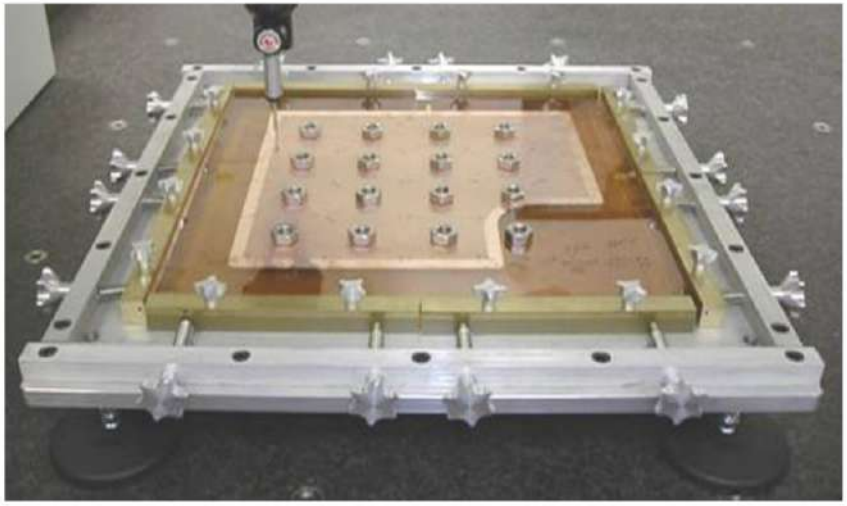

Measure of the **bending of a GEM foil**,
previously stretched at 20 MPa,
when a distributed load of 0.8, 1.6 and 2.4 N are applied

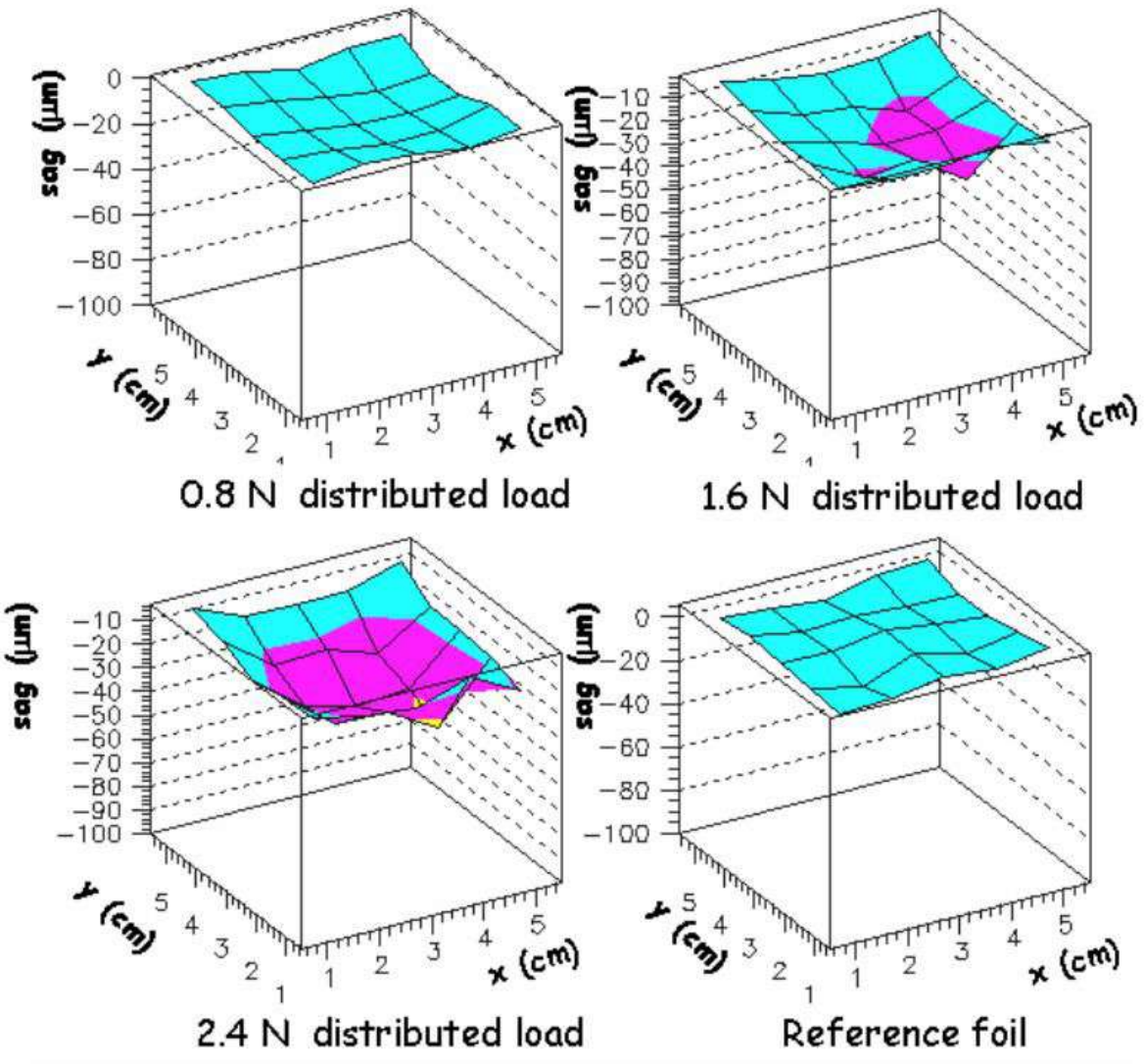

Radiation effect on the mechanical stretching

The radiation effects on the mechanical stretching of the GEM foil and the epoxy resin, used to glue the GEM on the fiberglass frame,
have been studied at the γ irradiation facility of the ENEA Casaccia.

For this test, a 20×24 cm^2 GEM foil has been stretched at 20 MPa and then framed.
To characterized the GEM foil before the test, a distributed load of 1 N,
corresponding to a mechanical pressure of 20 Pa, has been applied,
resulting in a sag of ~95 μm.

After 10 days of irradiation at 20 Gy/h (equivalently to 4 years of LHCb),
a sag of 120 μm has been measured for a mechanical pressure of 20 Pa.

Therefore, a mechanical tension loss of ~ 20% has been observed at the end of the test, which in our case correspond to a negligible effect

Mechanical variation

The uniformity of the chamber performances, such as the efficiency and the gas gain, depends on the mechanical tolerance on each gap.

In fact, since the tolerance on the GEM hole diameter
is by construction very tight, ± 2.5 μm,
and the gas gain saturates for the hole range of 40÷70 μm,
the effect on the gain due to hole diameter disuniformity is practically negligible.

Taking into account the planarity of the PCB panels, the possible disuniformity of the various gluing, the precision of the frame thickness, we estimate a global mechanical tolerance of ~100 μm for each gap of the chamber.

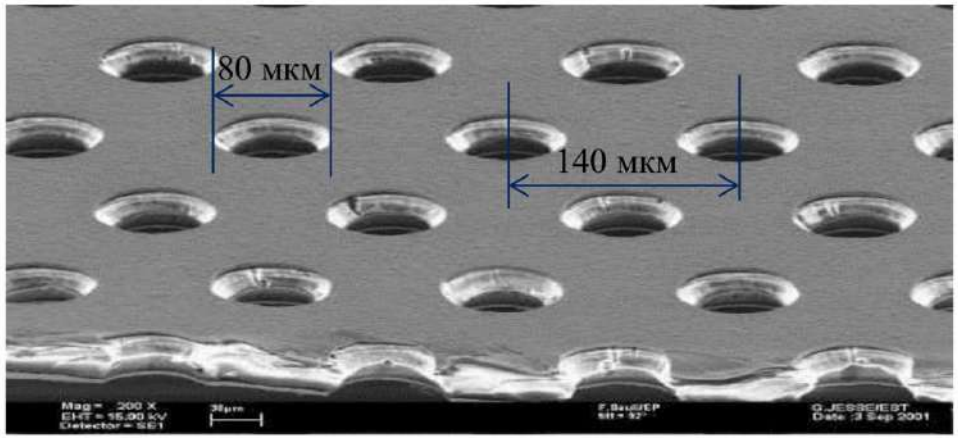

Gap width variation

Effective gain of a GEM detector is the product of the intrinsic gain and the electron transparency, which depends on the electric field inside the GEM holes and the electric field of the various gaps.

Since the electric field can be assumed constant across the gap, its value is done by the ratio of the voltage difference applied to the electrodes and the thickness of that gap (V/d).

Therefore, a local variation of the gap thickness (δgap) will correspond to a variation of the electric field in the gap (δE gap) and consequently to a variation of the effective gain, δG_{eff} , through the changes induced on the electron transparency, T :

$$\delta gap \implies \delta E_{gap} \implies \delta T \implies \delta G_{eff}$$

Since the effective gain represents the charge collected on the the pads readout, the measurements of the effective gain has been performed measuring the current induced on the pads.

Gap width variation

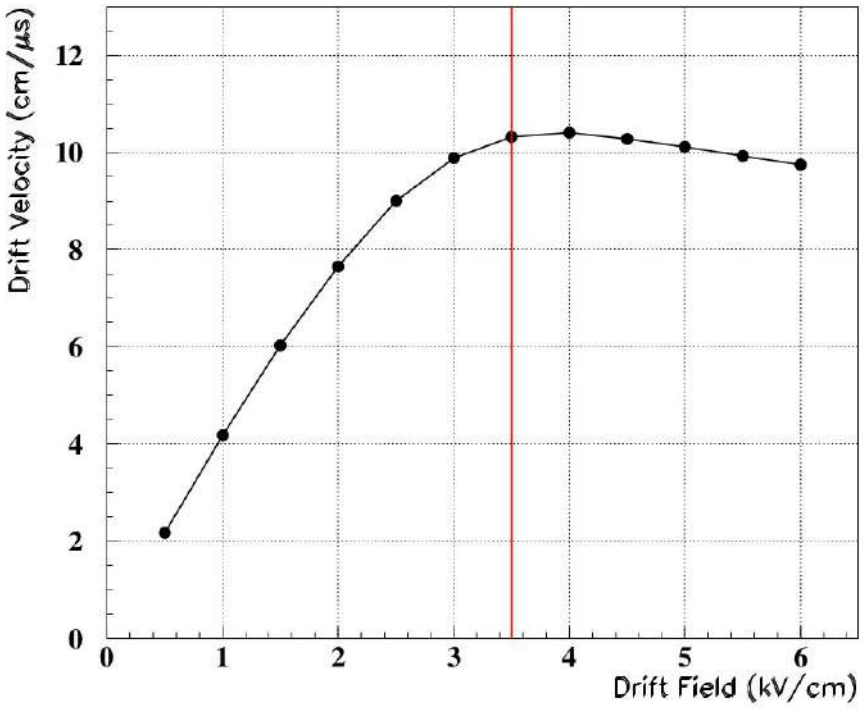

Electron drift velocity as a function of the drift field for $Ar/CO_2/CF_4$(45/15/40) gas. The maximum drift velocity is reached when the drift field is set at 3.5 kV/cm

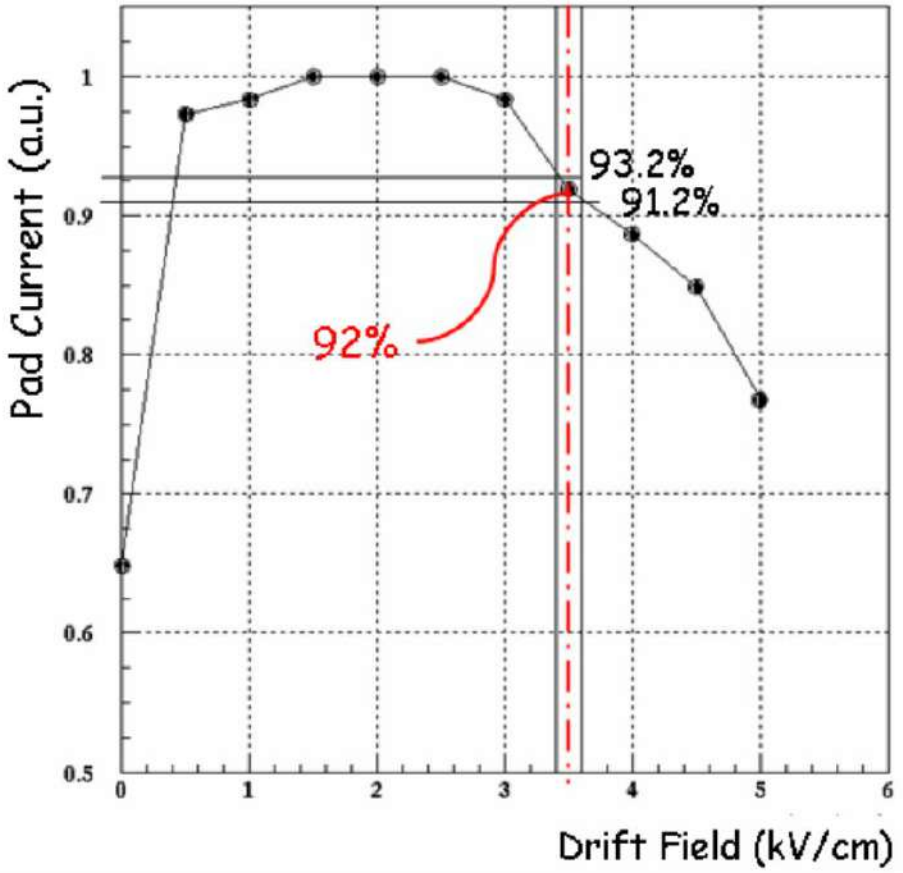

Normalized pad current of the detector as a function of the drift field. The red dotted line indicates the value chosen for the drift field, while the black lines indicate the range of variation (±0.1 kV/cm) corresponding to a mechanical tolerance of ± 100 μm. The resulting effective gain variation (δG drift) is ± 1%.

Влияние вариации толщины промежутков на вариации коэффициент газового усиления

	Gap Thickness [mm]	E_{field} [kV/cm]	δE_{field} (δ gap = $\pm$ 100 μm) [kV/cm]	δG_{eff} [%]
Drift	3	3.5	0.1	1
1^{st} transfer	1	3.5	0.35	3
2^{nd} transfer	2	3.5	0.18	3
Induction	1	5.0	0.5	4
			Total $\Delta\, G_{eff}$	*6*

Summary of the gain variation due to a mechanical tolerance of $\pm$ 100 μm in each gap of the detector.

Conclusions on full size detector investigations

The full size detector operated with the fast $Ar/CO_2/CF_4$ (45/14/40) gas mixture, demonstrate to be suitable to operate in the harsh environment around the beam pipe and largely fulfills the requirements of the region M1R1 of the LHCb experiment

The full size detector, constituted by two coupled 20×24 cm^2 triple-GEM detectors, have been extensively and successfully tested at the T11-PS CERN facility, confirming the results obtained in the R&D phase with the small prototypes

A novel GEM foil assembly technique based on the stretching of the GEM foil itself was developed

The detector construction does not show any critical points
and the construction of the 24 triple-GEM detectors has been started
in the two INFN production sites of Cagliari and Laboratori Nazionali di Frascati

После апгрейда 2018 - 2022 годов

станцию M1 из детектора LHCb **убрали**

Side view of the LHCb upgrade detector.

The Scintillating Fibre Tracker will be installed

in the tracking stations located downstream of the LHCb dipole magnet

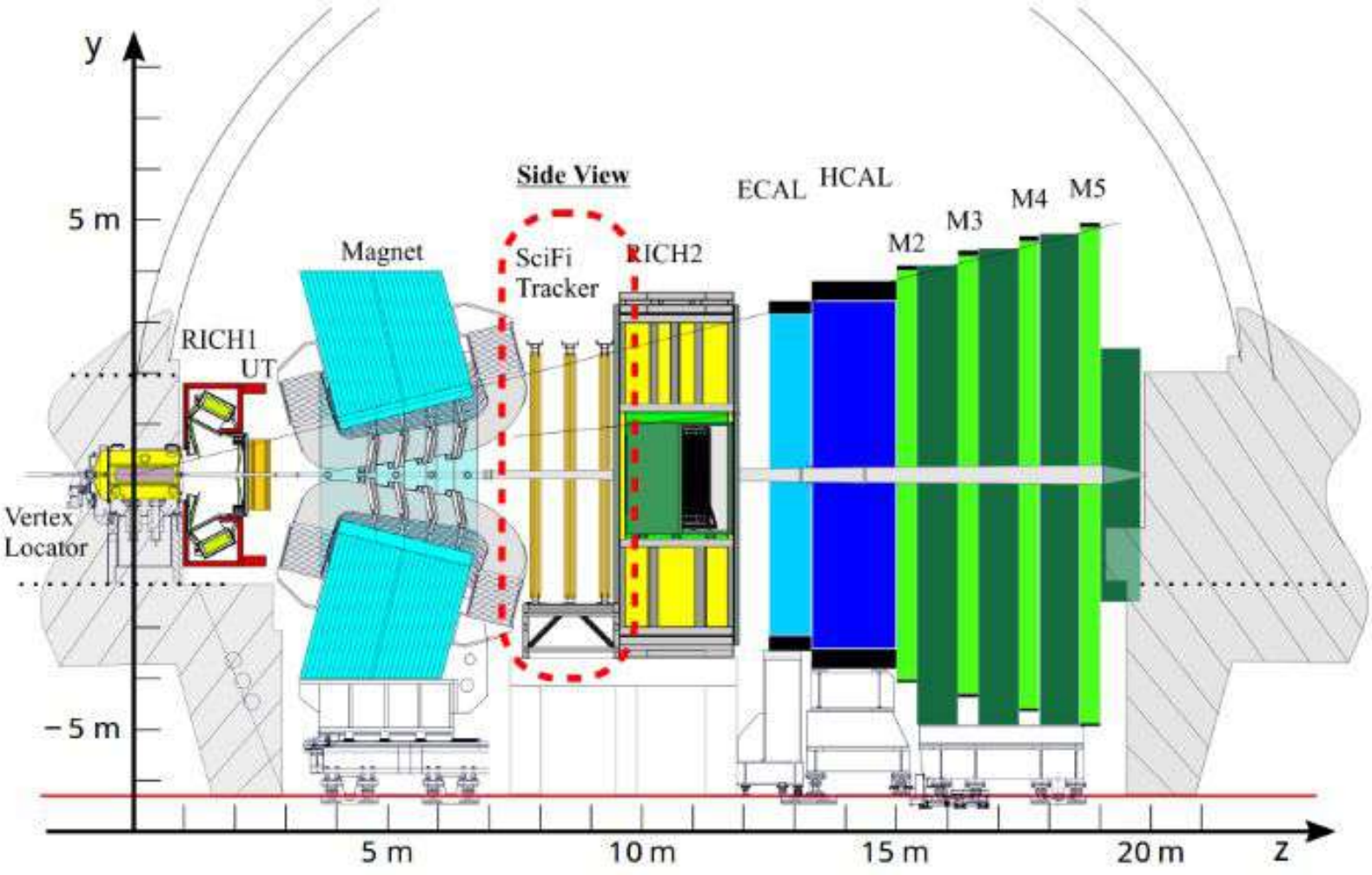

Масштаб времени

2000 – 2008 Строительство LHC

2008 – 2010 Настройка ускорителя

2010 – 2013 Run 1

2013 – 2015 Long Shutdown 1

2015 – 2018 Run 2

2018 – 2022 Long Shutdown 2

2022 – 2026 Run 3